Analysis and interpretation of roadway weather data for winter highway maintenance

by

David Scott Knollhoff

A thesis submitted to the graduate faculty

in partial fulfillment of the requirements for the degree of

MASTER OF SCIENCE

Major: Meteorology

Major Professors: Eugene S. Takle and William A. Gallus, Jr.

Iowa State University

Ames, Iowa

2001

Graduate College
Iowa State University

This is to certify that the Master's thesis of

David Scott Knollhoff

has met the thesis requirements of Iowa State University

Signatures have been redacted for privacy

DEDICATION

I would like to dedicate this project to Mr. Arthur Moser. Arthur was my junior college mathematics teacher in Illinois during the early 1990s. He is my beloved friend, my spiritual mentor, and my brother in Christ. I can't even begin to count the hours of free mathematical aid and spiritual guidance he gave to me! He not only helped me to pursue my goal of becoming a professional meteorologist, but he taught me to pursue my goal in such a way that my Lord Jesus Christ would be glorified through all my audible words and through my daily interactions with others (Colossians 3:17) that I would meet along the path of life. I look forward to the day when I can give back to someone the gift that I have been given by God – an ordinary man with extraordinary wisdom to share. Thanks, Mo. I love you, and you are in my thoughts daily.

TABLE OF CONTENTS

LIST OF FIGURES

LIST OF TABLES

ABSTRACT

Formation of ice and frost on pavement surfaces presents a potential hazard to the motoring public in cold climates. Pavement temperatures are not measured routinely by the National Weather Service and are not part of public forecasts of winter conditions, but highway maintenance personnel must make frost suppression and anti-icing decisions based on expectations of future pavement temperatures. The Road Weather Information System measures pavement, air, and dew point temperatures, pavement conditions, and wind data at numerous locations in the state of Iowa and reports the data in real-time to maintenance offices. The surface and near-surface data from the road weather system were analyzed to develop winter weather forecast procedures to compliment anti-icing techniques already practiced within the Iowa Department of Transportation.

Nocturnal pavement temperatures as reported by temperature sensors located in and near Des Moines and Cedar Rapids were analyzed under different classifications of cloud cover and for seasonal variations. Results show that the urban pavement temperatures near both Des Moines and Cedar Rapids are generally higher than rural pavement temperatures under different sky conditions. The heat island impact on surface temperatures in Des Moines was found to be slightly larger than that of Cedar Rapids. Pavement temperature cooling patterns differed among the months analyzed, and the roadways had different cooling characteristics compared to the bridge decks.

A model based on simple concepts of moisture flux to the surface was developed that uses current road weather data and forecasts of dew-point temperature, air temperature, surface temperature, and wind speed to calculate frost accumulation on bridge decks in Iowa. The analysis showed that the model has sufficient accuracy to be used as an operational tool to forecast bridge deck frost. A logistical regression procedure was developed to determine the probability that a maintenance worker will observe frost for a given calculated frost depth.

CHAPTER 1. INTRODUCTION

From late autumn through early spring, the formation of frost on roadways and bridges is a hazard to motorists in Iowa. Consequently, the Iowa Department of Transportation (IaDOT) suppresses frost formation. IaDOT maintenance personnel receive site-specific road weather forecasts to warn them on the timing details of frost events. Highway maintenance personnel use anti-icing and deicing techniques to battle frost formation based on the prediction of future road surface temperatures (RSTs) and road surface conditions (RSCs) provided in the road weather forecasts. In addition to site-specific road weather forecasts, IaDOT maintenance personnel use real-time road surface temperature and atmospheric temperature data measured by Roadway Weather Information System (RWIS) sensors to monitor atmospheric and pavement temperature trends. These data are collected and archived by the IaDOT.

In order to effectively combat the formation of frost on roadways and bridge decks during the cold season, research on icy road events in Iowa is needed for many reasons. First, Iowa RWIS stations are a fairly new addition to the IaDOT (late 1980s), and they have been recently (1998) upgraded to a new statewide computer environment. Consequently, the ability to access large amounts of RWIS data provides a valuable resource for numerous maintenance decisions needed for Iowa roads during frost events. Real-time RWIS data are used to refine the timing details of when to activate anti-icing and deicing procedures on paved roads. Secondly, only one study (Takle, 1990) on pavement frost has been completed in Iowa. Takle (1990) showed that a total of 2608 bridge and 1615 roadway frost observations occurred for the winters from 1985 to 1989. He concluded that the number of bridge frost events ranges from about 12 to 58, and that the number of roadway frost events varies from about 7 to 35 across Iowa per year. This study revealed that frost frequently forms on paved surfaces in Iowa. Thirdly, accurate prediction of winter RSTs and RSCs leads to economic, environmental and human benefits (Thornes, 1989) notably safer roads, fewer anti-icing runs, less rust damage to cars and bridges, and reduced waterway pollution. Lastly, the depth of frost accumulation and

the length of time frost is being deposited on paved surfaces are not easy variables to measure. Thus, predictive models have been developed to predict RSTs and the absence or presence of frost on bridges and roadway networks. Despite substantial improvements in understanding ice formation on roadways (Bogren and Gustavsson, 1989), continued research is needed to improve predictive models.

The goals of this study are to address this need for pavement temperature analyses in Iowa during the IaDOT winter maintenance season (October 15 through April 15) and to improve the prediction of frost formation around Iowa. The first objective is accomplished through analyses of nocturnal pavement temperature trends in Des Moines and Cedar Rapids. The second portion of this thesis gives the results on the prediction of frost accumulation on bridges by the use of a prognostic frost model and reports the results on the probability of a human observing a predicted frost depth.

CHAPTER 2. LITERATURE REVIEW

Because the northern latitudes of North America and Europe experience frequent snow, sleet, ice, and frost events during the cold season, the impacts of these conditions on highway safety have stimulated numerous studies of road surface temperatures and winter road conditions. RSTs and RSCs have been studied more heavily in Europe than anywhere else. In part, this fact arises because Europe had a well established automated road weather network in use by the mid 1980s, unlike the United States and Canada which began their RWIS networks in the late 1980s. Recent European research has been focused on the controlling factors of road surface temperature changes, on the prediction of RSTs and RSCs at site-specific road locations and along road networks, and on the prediction of frost formation on pavement surfaces.

2.1. Winter road surface temperature and road condition analyses

Road temperatures can vary greatly across a road network, even within city limits (Hewson and Gait, 1992). Topography is one of the most important factors controlling the variation of RSTs along a road network. Shao et al. (1998) concluded that RSTs varied up to 10°C –12°C along a large mountainous road network having large variations in altitude in Nevada. He also stated that, generally, a decrease of RST was observed with an increase in altitude. A study by Bogren and Gustavsson (1991) showed that valley geometry affected nocturnal pavement temperatures. They related the intensity of air temperature cold pools to the width and depth of valleys in Sweden. They concluded that air temperature differences between a valley and surrounding areas increased with increasing depth and width and that an increase in cold air pool intensity of 1°C lowered the RST by 0.4°C during nocturnal hours. Gustavsson (1990) described how the prevailing wind speed influenced pavement temperature variations in the county of Skaraborg in Sweden. He found variations to be low with 2-m wind speeds higher than 4 m s^{-1} to 5 m s^{-1}. Another factor that affected nighttime RSTs was whether or not the road surface was screened by objects (i.e., trees, buildings, hills) in the daytime (Bogren, 1991). He concluded that the RST differences between a screened site and an exposed site

during the day, due to the sky-view factor, influenced RST differences at those sites after sunset.

Most prognostic roadway weather models in use today give site-specific forecasts where RWIS sites are located. Real-time RWIS data from site-specific locations are used for initializing model runs. Different RST models have been tested for site-specific locations in western Europe (Rayer, 1987; Sass, 1992; Shao and Lister, 1996; Thornes and Shao, 1991). Rayer (1987) developed one of the first operational RST numerical models which predicted pavement temperatures for RWIS sites across the United Kingdom. His model included schemes that considered the effects of clouds, rain, and changing solar declination. The United Kingdom Meteorological Office first used the model in November 1986 as an advisory tool for road maintenance engineers during the winter of 1986-1987. This study encouraged an expansion of analyses on RSTs and the need for better prediction tools. Thornes and Shao (1991) looked at the interrelationships between RST and geographical road construction and meteorological inputs using the Icebreak model (Shao, 1990). Sensitivity tests using the Icebreak model showed that air temperature, cloud amount and cloud type were the most important factors that influenced the variation of RSTs at road weather sites. They also concluded that the influences of dew-point temperature, wind speed, and the thermal properties of the pavement were small. Sass (1992) tested a prognostic road condition forecast model developed at the Danish Meteorological Institute (DMI). This model was tested at a Danish road station, where the model assumed that the road was fully exposed to sunshine. He found that the best results in predicting RSTs and RSCs were obtained with detailed air temperature and humidity analyses taken from radiosonde data. Because large model sensitivity was found using atmospheric input data, Sass suggested that this model should be coupled to a realistic atmospheric forecast model to get the best road surface results. The test results indicated that the model could be used for high-quality RST forecasts up to 3 h. Shao and Lister (1996) developed an automated road ice prediction model that provided short-term (up to 3 h) high-

accuracy forecasts of RSTs and RSCs. Their model is unique in that it is the only fully automated physical road ice prediction model that requires no external meteorological input data other than automatically collected sensor measurements of surface temperature, air temperature, dew-point temperature, and wind speed from site-specific RWIS forecast sites. Results showed that their technique is acceptable for short-term forecasts. They concluded that over 95% of 3-h minimum temperature forecasts have an error of $\leq 2°C$. However, model performance becomes poorer as the forecast period gets longer.

RWIS sites monitor pavement temperature trends only at certain spots along roadway networks. Other tools to monitor pavement temperature trends and conditions are used for entire road networks. Thermal mapping is one widely used technique to record and quantify patterns of RSTs along such networks. Thermal mapping is a useful tool to provide an economic, easy, effective and accurate way to describe and display the actual spatial variations of RSTs for road networks (Shao et al., 1997). A local climatological model (LCM) is another tool used to predict RSTs and RSCs along entire stretches of road. In summary, the authors (Bogren et al., 1992; Gustavsson and Bogren, 1993) concluded that such tools as RWIS sites, thermal mapping and LCMs enhanced the prediction of RSTs and RSCs.

2.2. Frost formation on roadways and bridges

Studies on the controlling factors of frost formation on roadways and bridges have been completed by Gustavsson (1991) and Gustavsson and Bogren (1991) during warm-air advection events. Gustavsson and Bogren (1990) concluded that the spatial distribution of slipperiness in Sweden was dependent on two weather scenarios preceding the warm-air advection. First, if clear and calm conditions existed before the advection event, large local temperature differences due to variations of topography highly influenced how rapidly frost formed. Considerable time differences for the onset of slippery conditions between adjacent sites were likely. Secondly, the effect of local topography was not as important when the warm front was preceded by cloudy, windy conditions. Variation in temperature decreased under

these weather conditions. Therefore, the controlling factor of frost formation and road slipperiness was the progressing frontal movement. In addition to preceding weather scenarios and local topography Gustavsson (1991) added that the thermal properties of the road surface were another factor influencing road slipperiness during warm frontal passages. He concluded that materials used in the roadbed influenced the warming rate of the pavement surface, especially during warm-air advection events preceded by cloudy, windy conditions.

Convincing arguments (Thornes, 1989) by meteorologists who specialize in winter road conditions support the continued use and development of ice prediction models. Thornes (1996) proved that savings occurred for winter road maintenance, and unnecessary road salting would occur less often with the use of accurate road condition models. The latest advances in modeling slippery pavement surfaces (Barker and Davies, 1990; Hewson and Gait, 1992; Sass, 1992 and 1997; Shao and Lister, 1996; Takle, 1990) showed the need for further research and development of prognostic systems. Thus, this study extends pavement temperature analyses and explores the possibility of improved frost forecasts for the state of Iowa.

CHAPTER 3. PAVEMENT TEMPERATURE ANALYSIS

3.1. Introduction

Nighttime pavement temperatures as reported by site-specific RWIS sensors located in and near Des Moines (DSM) and Cedar Rapids (CID) were analyzed under different classifications of cloud cover. One difficulty in the use of site-specific pavement temperature data is the question of how representative measurements made at one location are for other roadways and bridges in the vicinity. To address this question, differences between nocturnal urban and rural patterns of temperature and temperature changes under different types of cloud cover are analyzed in this chapter and reported for DSM and CID. A sharp decrease in temperature from early evening to early morning as shown in Figure 1 is a typical winter pattern of observed roadway temperatures for DSM, with clear sky conditions (solid black line) giving the most extreme rate of temperature decrease. Because the cooling part of the temperature-change cycle is most critical for winter maintenance decisions, the analysis focuses on nocturnal pavement temperature behavior from early evening (1800 LST) to early morning (0700 LST). Also, this study analyzed seasonal variations in pavement temperatures under the different types of cloudiness.

3.2. Data

Pavement temperature data for the months of October 1996 (OCT 96), December 1996 (DEC 96), January 1997 (JAN 97), April 1997 (APR 97), and October 1997 (OCT 97) from the RWIS sites in Des Moines and Cedar Rapids were extracted from the IaDOT archives and used in this study. Because of many consecutive days of missing pavement temperatures, all data from both sites for the months of November 1996 and February 1997 were excluded from the analysis. Also, October 1996 RWIS data for CID were excluded from the analysis due to numbers that were physically unrepresentative compared to data from surrounding RWIS sites.

Cloud cover data for Des Moines and Cedar Rapids were obtained from the 1996 and 1997 Local Climatological Data (LCD) records maintained by the National Climatic Data

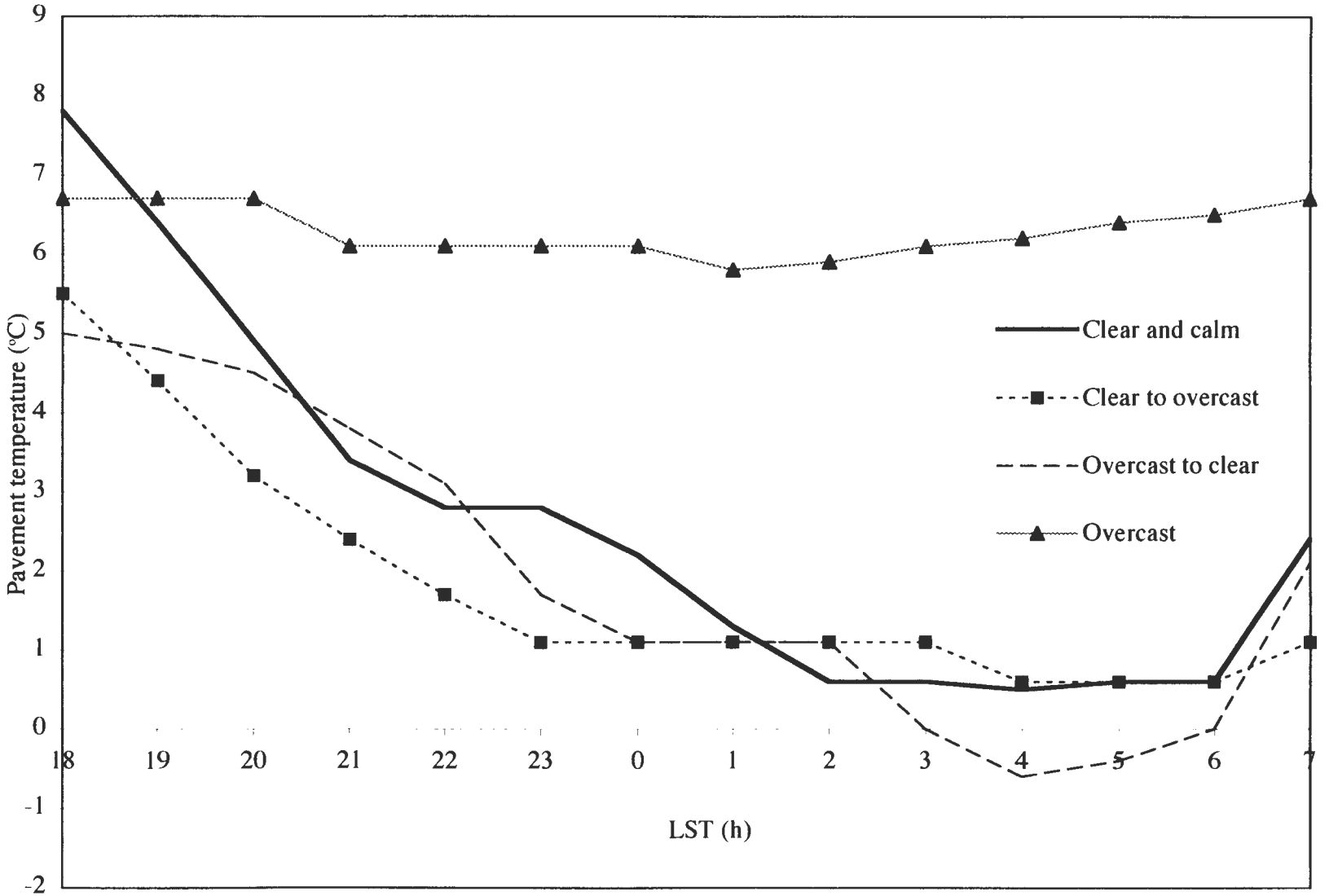

Figure 1. Southwest Des Moines roadway pavement temperatures for the 96/97 winter season.

Center and local airport ASOS weather sites maintained by the National Weather Service.

3.3. RWIS locations and site characteristics

Des Moines and Cedar Rapids each have two RWIS sites, one located generally southwest of the highly populated urban area and the other downtown. The downtown DSM site has three pavement temperature sensors located in the vicinity of the Des Moines River on I-235. The southwest DSM site has four pavement temperature sensors located over the Raccoon River and Highway 5. The downtown CID site has four pavement temperature sensors located on I-380 in the vicinity of the Cedar River. The southwest CID site is located on US Highway 30 near a railroad overpass, and it also has four pavement temperature sensors. The pavement sensors at all RWIS sites are cemented securely into the concrete/asphalt roadway approaches (RA), bridge decks over land (BL), and/or bridge decks over water (BW). Table 1 includes the DSM and CID RWIS site and sensor locations.

The DSM southwest RWIS site is located in a low lying, relatively flat, open area near Hwy–5 and I-35/80. Gentle rolling hills surround the site. The terrain slopes down moderately toward the RWIS tower. Small trees and vegetation are located close and large trees exist

Table 1. RWIS sites and sensor locations.

Cedar Rapids, Iowa							
Downtown				Southwest			
Sensor	Route	Direction	Type	Sensor	Route	Direction	Type
1	I-380	N/B	BW	5	Hwy-30	W/B	BL
2	I-380	S/B	BW	6	Hwy-30	E/B	BL
3	I-380	N/B	BL	7	Hwy-30	E/B	RA
4	I-380	Ramp	RA	8	Hwy-30	E/B	BL
Des Moines, Iowa							
Southwest				Downtown			
Sensor	Route	Direction	Type	Sensor	Route	Direction	Type
1	Hwy-5	W/B	BL	5	I-235	W/B	RA
2	I–35/80	N/B	BW	6	I-235	E/B	BL
3	Hwy–5	W/B	RA	7	I-235	W/B	BW
4	I–35/80	S/B	BW				

RA: roadway approach; BL: bridge deck over land; BW: bridge deck over water;
N/B: northbound lane; S/B: southbound lane; E/B: eastbound lane;
W/B: westbound lane

mainly farther away. No large residential, commercial, industrial, or building complexes are within 5 km of the site. This site is located in the Raccoon River valley and is susceptible to cold air pooling. The downtown site is located just east of the Des Moines River on I-235. The terrain slopes down from westerly directions toward the site and slopes upward in eastward directions away from the site. Screening effects by trees and buildings may be a factor in pavement cooling, especially during the morning hours before and a little after sunrise and during the evening. Large buildings and trees, residential, and commercial areas are within 0.5 km, especially west of the site. Smaller buildings and trees exist eastward. In general, the buildings and large amounts of concrete probably act as a source of heat, especially during the nocturnal hours.

In the southwest part of Cedar Rapids on Hwy 30, an RWIS site is located near the Archer Daniels Midland (ADM) plant. The RWIS tower is placed in a relatively high spot compared to its surroundings, especially toward easterly and southerly directions. Large buildings and trees and large commercial and industrial areas are relatively close to the site, within 0.5 km. Even though no water bodies exist near the site, the ADM plant acts as a source for heat and moisture. These characteristics would help to inhibit cold air pooling. The southwest site is located away from downtown Cedar Rapids, but it remains in a fairly urbanized location. The downtown tower is placed on I–380 close to the Cedar River and within the river valley. Large trees and small buildings and commercial areas surround the tower within 0.5 km. Flat terrain is common close to the tower. Otherwise, gently rolling hills exist in most directions except to the south.

3.4. Procedure

Because the collected RWIS data were recorded at irregular intervals (5 min to 3 h), a linear interpolation procedure was used to produce an hourly temperature dataset. This dataset served as the basis for computing monthly pavement temperature differences, cooling rates, and lag times between the downtown and southwest RWIS sites.

Oke (1978) used a simple expression to describe a horizontal temperature difference (1) between urban and rural locations. This same expression was used for computing pavement temperature differences between the downtown and southwest RWIS sites for both cities. The temperature difference expression is given by the following equation:

$$\Delta T = D - SW \quad (1)$$

where D is the downtown RST and SW is the southwest RST. Equation (1) represents the magnitude of the difference between the downtown site RST and the southwest site RST for RA, BL, and BW sensors in this study. Cooling rates for RA, BL, and BW were computed by subtracting the RST at one hour from the value one hour earlier over the nighttime. Average monthly ΔT and cooling rates were computed and stratified according to the absence or presence of cloud cover and cloud-cover change. The four different cloud cover classifications were (i) clear skies and calm conditions (winds ranging from 0 m s^{-1} to 2.5 m s^{-1}), (ii) transition from overcast to clear skies, (iii) transition from clear to overcast skies, and (iv) completely overcast conditions. Maintenance personnel may be able to take advantage of the magnitude of ΔT in refining the timing of downtown roadway treatments. For instance, if the time of ice formation due to pavement cooling at the southwest site is noted, the downtown RST and cooling rate can be used to predict the time of freezing at downtown sites. By dividing the average monthly value of ΔT by the average monthly downtown cooling rate, an estimated mean lag time for the downtown location to cool to a threshold temperature of its southwest counterpart is obtained and stratified per month according to the different classifications of cloud cover.

For each month, both cities contained from 1 to 10 cases per cloud-cover classification. Each case included 13 interpolated hourly observations (1800 LST to 0700 LST) used to compute averages and standard deviations. Overall, the total number of nocturnal cooling hours analyzed was 1079 h out of a possible 1200 h for Des Moines and 1014 h out of a possible1130 h for Cedar Rapids. Archived surface maps were used to determine large-scale

weather events (i.e. frontal passages, warm-air advection, and cold-air advection) over Iowa. Periods when major changes in large-scale weather events were the dominant influence on changes in pavement temperature (10% of total hours analyzed) were excluded from the analysis.

Wind speed, wind direction, precipitation, roadway subsurface temperature, construction material of the roadways and bridges, traffic flow, and temperature variations along the road networks between the downtown and southwest sites were not taken into account in this study. However, it is important to note three factors that may have influenced pavement temperature cooling in this study. First, the wind speeds observed in this study for all classifications of cloudiness except clear/calm cases ranged from a minimum of 2.5 m s^{-1} to a maximum of 12.7 m s^{-1}. Secondly, when overcast conditions dominated the nocturnal period, a few hours of precipitation were occasionally observed. These hours of precipitation were not excluded in the study. Lastly, it is assumed that snow does not cover the sensor at the four sites during the test period.

3.5. Analysis of pavement temperatures at RWIS sites in Des Moines

3.5.1. Pavement temperature differences

Figure 2 shows an example of pavement temperature cooling for the roadways and bridge decks at the RWIS sites in Des Moines under clear skies and calm conditions. This graph points to the fact that temperature differences of up to 5°C are possible between comparable sensors from the two different sites during the nighttime. This result corroborates the result of Shao et al. (1998). However, the temperature trend in Figure 2 is influenced very little by topographical differences. Table 2 gives the average monthly and standard deviation values of ΔT between the downtown and southwest RWIS sites in Des Moines, stratified under different classifications of cloud cover.

During autumn, winter, and spring months, positive values of average nighttime ΔT indicated that the downtown RSTs were warmer than their counterpart southwest RSTs under

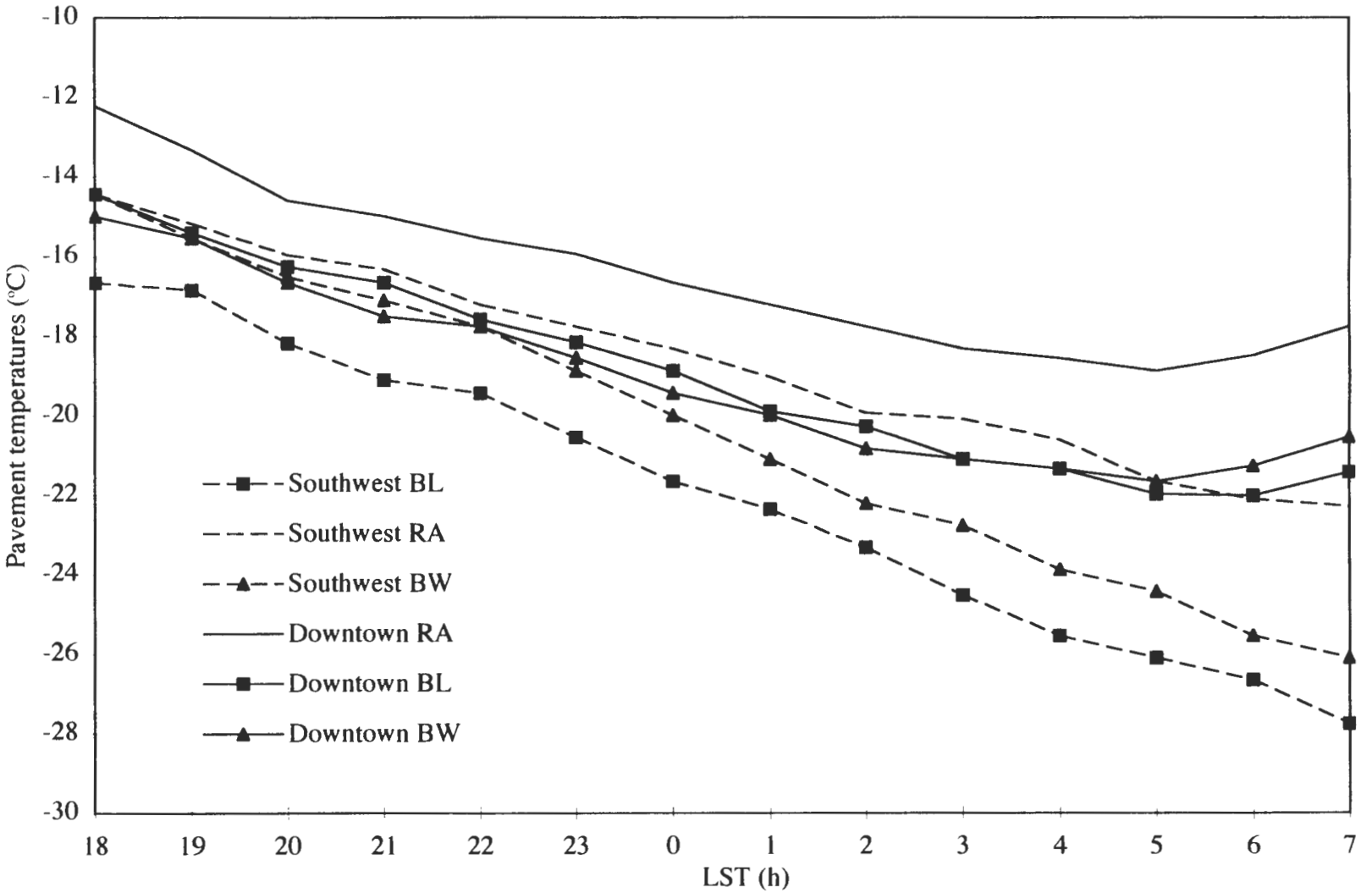

Figure 2. DSM RWIS pavement temperatures (01/13/97).

Table 2. Average and standard deviation [in brackets] of ΔT (°C) in Des Moines.

	Clear/calm			Overcast to clear			Clear to overcast			Overcast		
	RA	BL	BW	RA	BL	BW	RA	BL	BW	RA	BL	BW
OCT 96	1.3 [1.1]	1.6 [1.5]	1.3 [1.0]	1.3 [0.9]	1.6 [1.2]	0.8 [0.8]	1.3 [1.0]	1.0 [0.8]	0.8 [0.7]	0.7 [0.3]	0.1 [0.3]	0.4 [0.3]
DEC 96	1.7 [0.8]	1.7 [0.8]	0.8 [0.8]	1.2 [0.7]	1.4 [0.6]	0.6 [0.6]	1.1 [0.8]	1.1 [0.4]	0.3 [0.4]	1.1 [0.9]	1.1 [0.8]	0.3 [0.7]
JAN 97	2.2 [0.9]	1.3 [1.4]	1.6 [1.3]	1.1 [0.6]	1.4 [0.8]	0.8 [0.8]	1.4 [1.1]	0.7 [0.4]	0.8 [0.8]	0.9 [0.9]	0.8 [0.6]	0.7 [0.7]
APR 97	0.8 [1.2]	0.7 [1.6]	0.9 [0.8]	0.6 [0.7]	0.5 [0.8]	0.4 [0.6]	0.4 [0.9]	0.3 [1.2]	0.5 [0.9]	0.3 [0.9]	0.1 [1.0]	0.6 [0.6]

RA: roadway approach; BL: bridge deck over land; BW: bridge deck over water

all classifications of cloud cover, by magnitudes ranging from 0.1°C to 2.2°C (Table 2). The smallest average ΔT values and the largest standard deviation values occurred during APR 97. In all months average ΔT and standard deviation values indicated a nighttime trend in agreement with an urban heat island effect.

Average ΔT trends by cloud cover classifications can also be seen in the table. Generally, the largest temperature differences between the DSM RWIS sites existed under clear and calm conditions, less for transitions in cloud cover and least under completely overcast skies. Average ΔT values ranged from 0.7°C to 2.2°C for clear/calm conditions, 0.3°C to 1.6°C for transitions in cloud cover, and 0.1°C to 1.1°C for overcast conditions. Bridge decks generally had the smallest average ΔT values for most months and under most cloud cover classifications.

3.5.2. Cooling rates

The rate at which the pavement temperature cools during the nighttime is a significant factor in forecasting when wet surfaces might freeze. Table 3 shows the monthly averages and

Table 3. Average and standard deviation [in brackets] values of cooling rates (°C h^{-1}) for Des Moines.

		Clear/calm			Overcast to clear			Clear to overcast			Overcast		
		RA	BL	BW	RA	BL	BW	RA	BL	BW	RA	BL	BW
OCT 96	SW:	1.1 [1.3]	0.7 [1.1]	0.8 [0.6]	0.8 [0.8]	0.9 [0.8]	0.8 [0.6]	0.8 [1.4]	0.9 [1.2]	0.7 [0.8]	0.2 [0.4]	0.1 [0.4]	0.2 [0.4]
	D:	0.8 [1.1]	0.8 [0.9]	0.8 [1.0]	0.6 [0.9]	0.7 [0.9]	0.7 [0.8]	0.7 [1.0]	0.7 [1.0]	0.7 [0.9]	0.2 [0.3]	0.1 [0.4]	0.2 [0.4]
DEC 96	SW:	0.5 [0.6]	0.6 [0.6]	0.6 [0.6]	0.4 [0.6]	0.5 [0.6]	0.4 [0.6]	0.3 [1.1]	0.4 [0.5]	0.3 [0.5]	0.2 [0.5]	0.2 [0.7]	0.2 [0.5]
	D:	0.4 [0.6]	0.6 [0.6]	0.5 [0.6]	0.3 [0.7]	0.4 [0.6]	0.4 [0.7]	0.2 [0.6]	0.3 [0.5]	0.3 [0.5]	0.1 [0.5]	0.2 [0.5]	0.1 [0.4]
JAN 97	SW:	0.6 [0.6]	0.7 [0.5]	0.7 [0.6]	0.5 [0.7]	0.6 [0.7]	0.6 [0.6]	0.5 [0.7]	0.6 [0.8]	0.5 [1.4]	0.2 [0.6]	0.1 [0.6]	0.1 [0.4]
	D:	0.4 [0.7]	0.6 [0.6]	0.6 [0.6]	0.4 [0.6]	0.4 [0.6]	0.5 [0.7]	0.5 [0.7]	0.5 [0.8]	0.5 [0.7]	0.1 [0.5]	0.1 [0.4]	0.1 [0.4]
APR 97	SW:	1.4 [1.7]	1.5 [1.4]	1.2 [1.2]	1.1 [1.2]	1.1 [1.1]	1.0 [0.9]	1.2 [1.5]	1.2 [1.3]	1.1 [1.2]	0.6 [0.9]	0.6 [0.8]	0.5 [0.7]
	D:	1.2 [1.4]	1.1 [1.2]	1.2 [1.2]	0.9 [0.7]	0.9 [0.7]	0.9 [0.7]	1.0 [1.4]	0.9 [1.1]	0.9 [1.2]	0.5 [0.9]	0.4 [0.8]	0.5 [0.8]

RA: roadway approach; BL: bridge deck over land; BW: bridge deck over water; SW: southwest site; D: downtown

standard deviations of downtown and southwest site cooling rates for the RA, BL, and BW sensors under the different classifications of cloud cover. A positive rate revealed that the pavement surface was cooling, and a negative rate represented warming RSTs.

Overall, average cooling rates ranged from 0.1°C h^{-1} to 1.5°C h^{-1}, and average southwest cooling rates generally exceeded or infrequently equaled their downtown counterpart rates (Table 3). Also, a warming of the pavement surface occurred infrequently at times during the nocturnal hours for both DSM RWIS sites. Most of the warming events happened just before sunrise (0630 LST in October and 0530 LST in April). Figure 2 gives an example of warming RSTs before sunrise. At this time, the cause for the temperature rise is unknown, but is hypothesized to be early morning traffic.

Average bridge deck cooling rates equaled or exceeded RA rates by 0.2°C h^{-1} for most months under the different types of cloud cover. This suggests that the bridge decks reached a threshold temperature before their comparative roadways, so that they would reach freezing temperatures first. The smallest average rates existed in DEC 96, and the largest occurred in APR 97 (Figure 3). Yet, for APR 97, downtown/southwest RA rates generally equaled or exceeded their bridge deck rates by 0.1°C h^{-1} under the different classifications of cloud cover. Consequently, these observations for APR 97 suggest that the difference in subsurface heat fluxes between the downtown/southwest RA and their comparable bridge decks played a more important role during the spring/fall months than the winter months.

Cloud cover also affected cooling rates. The largest average cooling rates existed under clear skies and calm conditions, less for transitions in cloud cover and least under completely overcast conditions. An example of this cooling rate trend is shown in Figure 3. Cloud cover reduced heat loss to the atmosphere, while clear skies and calm winds allowed for an increase in heat loss from surface pavements. Cloud cover kept RSTs from falling quickly or even at all.

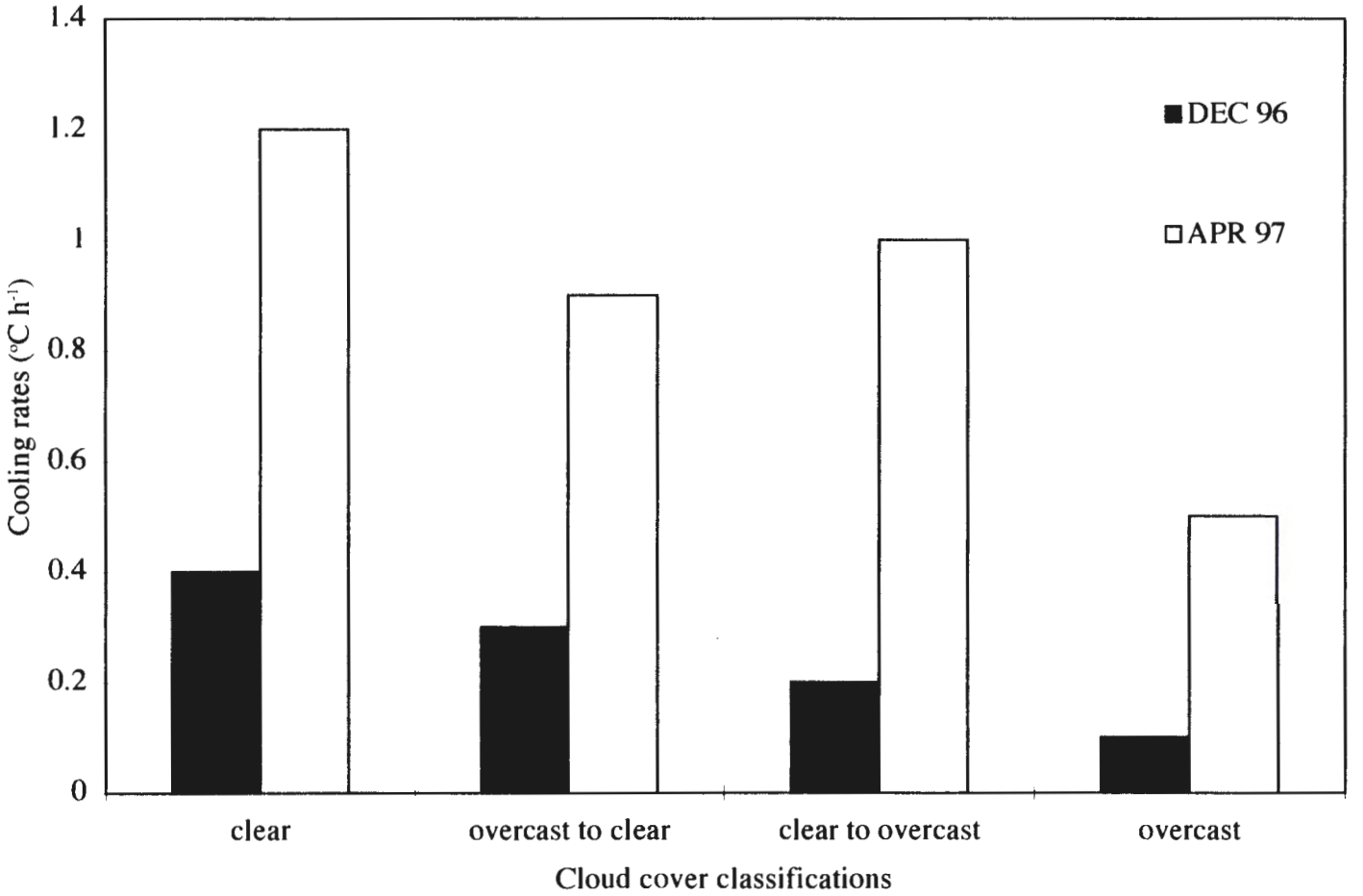

Figure 3. Downtown RA cooling rates in Des Moines for the different cloud cover classifications.

3.5.3. Mean downtown lag times

The mean downtown lag time is defined as the time it takes for the downtown roadway and bridge decks to cool to threshold southwest site temperatures (Table 4). For example, the mean downtown lag time for RA under a clear sky and calm winds in OCT 96 (1.6 h) was computed by taking the average ΔT for RA and diving that value by the average downtown RA cooling rate under the same cloud cover classification and month. However, it is possible that the downtown site may not cool to a threshold southwest site temperature. The southwest site would have to maintain significant cooling while the downtown site would not be able to cool. The conditions needed for such an event are nighttime overcast conditions over the metro, while the southwest site remained under clear and calm conditions. Because average downtown cooling rates were usually less than the average southwest site rates up to 0.2°C h^{-1}, the conditions needed for significant cooling differences were not often met. Thus, the downtown usually cooled to a threshold southwest temperature overnight.

Downtown lag times in Des Moines ranged from 0.3 h to 11 h. The longest lag times occurred during the winter months. When the average downtown cooling rates were small (DEC 96, JAN 97), long lag times existed for all classifications of cloud cover. APR 97 had the

Table 4. Mean downtown lag times (h) in Des Moines.

	Clear/calm			Overcast to clear			Clear to overcast			Overcast		
	RA	BL	BW	RA	BL	BW	RA	BL	BW	RA	BL	BW
OCT 96	1.6	2.0	1.6	2.2	2.3	1.1	1.9	1.4	1.1	3.5	1.0	2.0
DEC 96	4.2	2.8	1.6	4.0	3.5	1.5	5.5	3.7	1.0	11.0	5.5	3.0
JAN 97	5.5	2.2	2.7	2.8	3.5	1.6	2.8	1.4	1.6	9.0	8.0	7.0
APR 97	0.7	0.6	0.8	0.7	0.6	0.4	0.4	0.3	0.6	0.6	0.3	1.2

RA: roadway approach; BL: bridge deck over land; BW: bridge deck over water

shortest lag times because during that month average ΔT values were smallest and average downtown cooling rates were large compared to the southwest rates.

Overcast conditions allowed for the longest downtown lag times. Less heat was lost to space with overcast skies, which gave way to small downtown cooling rates and large lag times. Downtown locations took a longer time to hit a threshold southwest temperature, especially for overcast conditions. Because average roadway cooling rates were generally smaller than the average bridge deck rates, RA usually showed the longest lag times for most months and under most cloud cover categories.

3.6. Analysis of pavement temperatures at RWIS sites in Cedar Rapids

This analysis compared nighttime pavement temperatures between the two RWIS sites in Cedar Rapids for the different types of cloud cover. A period similar to the analysis performed for Des Moines is reported. OCT 96 data did not exist for Cedar Rapids, so OCT 97 data were used instead. The southwest RWIS site does not have a BW sensor because no river or water surface exists at that location. Consequently, temperature differences for BW were not evaluated. Data available for Cedar Rapids offered an independent comparison of calculated ΔT values, cooling rates, and mean lag times to the results from Des Moines.

3.6.1. Pavement temperature differences

Table 5 provides the average and standard deviation values of ΔT for the RA and BL sensors under the different classifications of cloudiness. Positive average values of ΔT show that downtown pavement temperatures were generally warmer (up to 1.4°C) than their counterpart southwest temperatures for all months and classifications of cloudiness. The magnitudes of average RST differences for Cedar Rapids were 0.2°C to 1.0°C less than those calculated between the two RWIS sites in Des Moines. Also, the lower average RST differences with large standard deviations indicate that southwest temperatures exceeded their downtown counterparts under all classifications of cloudiness more often compared to Des Moines.

Table 5. Average and standard deviation [in brackets] of ΔT (°C) in Cedar Rapids.

	Clear/calm		Overcast to clear		Clear to overcast		Overcast	
	RA	BL	RA	BL	RA	BL	RA	BL
DEC 96	0.6 [0.6]	0.5 [1.1]	0.0 [0.9]	0.1 [0.9]	0.6 [0.6]	0.9 [0.7]	0.4 [0.6]	0.4 [0.4]
JAN 97	0.9 [0.8]	1.0 [0.6]	0.2 [0.9]	0.4 [0.7]	0.8 [0.9]	1.4 [0.6]	0.2 [0.6]	0.4 [0.3]
APR 97	1.2 [0.8]	0.8 [0.9]	1.0 [1.0]	0.6 [0.9]	1.6 [1.0]	0.8 [1.3]	0.6 [0.7]	0.8 [0.4]
OCT 97	1.3 [0.8]	1.1 [0.7]	1.0 [1.0]	0.8 [0.6]	0.9 [0.7]	0.7 [0.7]	1.1 [0.7]	0.8 [0.6]

RA: roadway approach; BL: bridge deck over land

Average ΔT trends by cloud cover classifications can also be seen in Cedar Rapids. Generally, the largest magnitudes were observed for clear skies and calm conditions and the least under overcast skies. Average magnitudes of ΔT ranged from 0.5°C to 1.3°C for clear/calm skies, 0.0°C to 1.4°C for transitions in cloud cover, and from 0.2°C to 1.1°C for complete overcast conditions. This trend is similar to results from Des Moines but less in magnitude.

3.6.2. Cooling rates

Table 6 gives the average and standard deviation values of downtown and southwest cooling rates for RA, BL, and BW stratified according to the different classifications of cloudiness. Cooling rates ranged from 0.1°C h^{-1} to 1.2°C h^{-1} during the nighttime hours. Also, the downtown site cooled as quickly as or slightly faster than the southwest site for most months examined. This trend in cooling rates was opposite to that found in Des Moines. Similar to Des Moines, the largest average cooling rates in Cedar Rapids occurred under clear skies and calm conditions, with less for transitions in cloud cover and the least under completely

Table 6. Average and standard deviation [in brackets] values of cooling rates (°C h^{-1}) for Cedar Rapids.

		Clear/calm			Overcast to clear			Clear to overcast			overcast		
		RA	BL	BW	RA	BL	BW	RA	BL	BW	RA	BL	BW
DEC 96	SW:	0.3 [0.5]	0.4 [0.6]		0.5 [0.4]	0.6 [0.5]		0.2 [0.6]	0.3 [0.5]		0.1 [0.3]	0.1 [0.3]	
	D:	0.4 [0.4]	0.4 [0.4]	0.4 [0.5]	0.6 [0.5]	0.6 [0.6]	0.6 [0.6]	0.2 [0.6]	0.3 [0.4]	0.3 [0.6]	0.1 [0.4]	0.1 [0.4]	0.1 [0.4]
JAN 97	SW:	0.4 [0.4]	0.6 [0.6]		0.2 [0.5]	0.3 [0.6]		0.3 [0.6]	0.3 [0.6]		0.1 [0.6]	0.1 [0.5]	
	D:	0.5 [0.5]	0.6 [0.6]	0.6 [0.5]	0.3 [0.6]	0.3 [0.7]	0.3 [0.7]	0.3 [0.6]	0.3 [0.6]	0.4 [0.6]	0.1 [0.5]	0.1 [0.5]	0.1 [0.5]
APR 97	SW:	1.0 [1.3]	1.1 [1.3]		0.8 [0.9]	0.8 [1.0]		1.1 [1.4]	1.1 [1.3]		0.2 [0.8]	0.3 [0.8]	
	D:	1.1 [1.4]	0.9 [1.2]	0.9 [1.1]	0.9 [1.0]	0.8 [1.0]	0.7 [0.9]	1.2 [1.7]	1.0 [1.2]	1.0 [1.2]	0.2 [0.7]	0.2 [0.6]	0.2 [0.6]
OCT 97	SW:	1.0 [1.1]	1.1 [1.0]		0.6 [0.8]	0.7 [0.8]		0.9 [1.2]	0.9 [1.1]		0.4 [0.7]	0.4 [0.7]	
	D:	1.1 [1.3]	1.0 [1.0]	0.9 [0.9]	0.7 [0.9]	0.6 [0.8]	0.6 [0.7]	1.1 [1.2]	0.9 [0.9]	0.9 [0.9]	0.5 [0.2]	0.4 [0.8]	0.4 [0.8]

RA: roadway approach; BL: bridge deck over land; BW: bridge deck over water; SW: southwest site; D: downtown

overcast conditions.

Pavement temperatures either rose or didn't cool rapidly after 0430 LST under the different classifications of cloudiness. Early morning RST warming may have led to the large standard deviation values for the downtown and southwest site cooling rates. This warming was frequently observed, usually, an hour or two before sunrise. This trend was similar to that revealed in the Des Moines analysis. For Cedar Rapids in JAN 97, four out of five cases showed this warming trend under clear skies and calm conditions, eight out of ten for transitioning sky conditions and all three cases of completely overcast conditions. In total for JAN 97, 15 of 18 possible cases revealed that RSTs began to increase about two hours prior to sunrise. Other months showed similar results.

The data from APR 97 and OCT 97 revealed the largest average downtown and southwest site cooling rates under all classifications of cloudiness. For the winter months, the smallest average rates existed for all types of cloudiness. In general, results showed that the downtown cooling rates equaled or slightly exceeded their counterpart southwest rates up to 0.1°C h^{-1} under most cloud cover categories and most months. Also both roadway and bridge deck cooling rates were similar. These trends were opposite of the results from Des Moines.

3.6.3. Mean downtown lag times

Mean downtown lag times were stratified according to the cloud cover categories (Table 7). Downtown lag times ranged from 0.0 h to 4.7 h. These lag times were considerably less than those found from the analysis performed for Des Moines. DEC 96 and JAN 97 had the largest mean downtown lag times under most classifications of cloudiness. Similar to the results from the analysis for Des Moines, overcast skies produced the largest lag times in Cedar Rapids. Generally, the largest mean downtown lag times existed for the RA for most months and under most of the cloud cover categories. It took the downtown roadway RST a longer time to reach its counterpart rural RST than it did for the downtown BL RST to reach its southwest bridge deck temperature. In general, this suggests that the subsurface heat flux at the

Table 7. Mean downtown lag times (h) in Cedar Rapids.

	Clear/calm		Overcast to clear		Clear to overcast		Overcast	
	RA	BL	RA	BL	RA	BL	RA	BL
DEC 96	1.5	1.3	0.0	0.2	3.0	3.0	4.0	4.0
JAN 97	1.8	1.7	0.7	1.3	2.7	4.7	2.0	4.0
APR 97	1.1	0.7	1.1	0.8	1.3	0.8	3.0	4.0
OCT 97	1.2	1.1	1.4	1.3	0.8	0.8	2.2	2.0

RA: roadway approach; BL: bridge deck over land

downtown RA location allowed for the lower average cooling rates and the longest lag times.

3.7. Summary

The pavement temperature analysis concentrated on how the presence/absence, or change in cloud cover affected nocturnal pavement cooling patterns at RWIS sites located in Des Moines and Cedar Rapids. Temperature differences, cooling rates, and mean downtown lag times were computed for the roadways and bridge decks under different classifications of cloud cover. The analysis showed that downtown pavement temperatures near both Des Moines and Cedar Rapids are 2°C to 4°C higher than rural pavement temperatures under a clear sky but only 1°C to 2°C higher under cloudy conditions or when cloud cover is changing.

Results from Cedar Rapids were compared to the results from Des Moines. The population of Des Moines is approximately 200,000 and Cedar Rapids is around 100,000. Because the surface heat island in Des Moines was slightly larger than the one in Cedar Rapids (by 0.2°C to 1.0°C) and noting the population estimates, it appears that the urban effect is larger as cities get larger (Oke, 1982; Katsoulis and Theoharates, 1985). Consequently, RST trends for one city do not necessarily apply to another city.

RST cooling trends varied over time. The greatest pavement cooling was observed when relatively warm daytime temperatures were followed by rapid cooling at night. This trend was most common in the early (October) and late (April) months. Also, the roadways had different cooling characteristics compared to the bridge decks. In general, the bridge deck cooled faster than its counterpart roadway by 0.2°C h^{-1} in Des Moines. However in Cedar Rapids little difference in cooling rate trends between the roadways and bridge decks was observed.

It is important to note that the results from the pavement temperature analysis are preliminary since they covered only a few months. Winter, fall, and spring months from other years may give patterns that depart from the limited period studied here.

CHAPTER 4. PAVEMENT FROST ANALYSIS ON IOWA BRIDGE DECKS

4.1. Introduction

Frost frequently forms on pavement surfaces in Iowa during the cold season (October-April), particularly in the early morning under conditions of radiational cooling or warm advection. Frost accumulations may lead to hazardous conditions for motorists unless pavement surfaces are treated by chemical solutions. However, treating bridge decks with salt solutions every time the pavement temperature drops to the freezing point or below is not practical. For example, tax money pays for the salt used to suppress frost as well as the maintenance needed on roads damaged by chemical solutions. Also, owners of vehicles pay millions of dollars per year to fight automobile corrosion due to salt deposition on metal surfaces (Shao and Lister, 1996). In addition, salt pollutes the local environment by running off into the adjacent water sources and soil (Shao and Lister, 1996).

The Iowa Department of Transportation (IaDOT) chemically treats roadways and bridges for frost based on site-specific weather forecasts and real-time Roadway Weather Information System (RWIS) data. Current RWIS pavement temperatures alert IaDOT management personnel to freezing conditions at 51 locations across Iowa. Accurate frost predictions allow the IaDOT to maintain practical frost suppression programs, such as anti-icing and deicing procedures, and minimize negative environmental impacts.

In this study a simple numerical model is developed to predict the depth of frost accumulation on bridge decks. The model uses current RWIS data and forecasts of dew-point temperature, air temperature, surface temperature, and wind speed to calculate frost accumulation on bridge decks in Iowa. The model was tested and evaluated by comparing model-generated maximum frost depth with daily frost observations by IaDOT maintenance personnel. Curves of relative operating characteristics were used to evaluate the skill of the modeling procedure. A linear logistic regression technique was developed to determine the probability that a maintenance worker will observe frost at the predicted frost depth.

4.2. Data

4.2.1. RWIS data

Sensor data from five automated RWIS sites were extracted from the IaDOT data archives. Bridge deck pavement surface temperatures, 5-m wind speeds, 2-m air temperatures and dew point temperatures from RWIS sites in Spencer, Mason City, Waterloo, southwest Des Moines, and Ames, Iowa for 21 cold-season months (1995-1998) were used as model input. Each automated RWIS site has four to five surface sensors strategically embedded in the bridge decks. At each RWIS site, the bridge deck sensor that recorded pavement surface temperatures with the least missing data was used in the model prediction procedure.

4.2.2. Pavement frost observations

During the cold season, maintenance personnel record daily observations of the presence or absence of frost as viewed from inside a vehicle while making surveys of bridges. The daily surveys usually are taken between the hours of 0500 LST and 0700 LST. The frost observations are recorded on official winter maintenance sheets and then archived for litigation or research purposes. Four hundred sixty two frost observations for which corresponding RWIS data were available were used in the frost analysis for model verification.

4.2.3. Potential errors

No study is exempt from error in the collected data. The first potential error arises with the location of the RWIS atmospheric tower relative to the pavement surface. RWIS towers provide information relating to the pavement surface and snow and ice conditions on the roadway. However, they may not accurately represent large-scale conditions required for frost forecasting. The model assumes that the 2-m air temperature, 2-m dew point temperature, and the 5-m wind speed are measured directly above the pavement surface. In reality, the RWIS tower and its atmospheric sensors are a few meters removed from the pavement surface. Secondly, the atmospheric tower is often located at a lower or higher elevation than the adjacent pavement surface. Thirdly, the low level atmospheric RWIS data may be influenced by the local

environment such as grass, soil or snow cover. Finally, the atmospheric and pavement temperature sensors are accurate to ±0.3 °C over the temperature range of −30 °C to 50 °C. The wind speed sensing element is accurate to ±2.2 m s^{-1}.

The frost observations may also contain errors. Because the frost observations were recorded within a large range of time between 0500 LST and 0700 LST, the maintenance personnel may have missed actual frost deposition. The frost may have melted or sublimed before 0500 LST or may not have been observable until after 0700 LST. Also, maintenance personnel may have missed frost accumulations on pavement surfaces since observations are made from inside a vehicle.

4.3. Procedure

4.3.1. Linear interpolation

Automated RWIS sensor readings are recorded at irregular time intervals due to IaDOT internal software programming. The times between readings varied from 5 minutes to 3 hours. A linear relationship with time for temperature change and wind speed change was assumed between the readings, and a linear interpolation procedure was created to calculate one minute values from the original RWIS sensor readings taken at irregular intervals. The original RWIS data were first converted into one minute values using the linear interpolation procedure before model frost accumulations were calculated.

4.3.2. Frost formation on pavement surfaces

Frost formation on pavement surfaces is influenced by factors as wide-ranging as atmospheric conditions to the amount of traffic on roadways and bridge decks. Hewson and Gait (1992) showed that the meteorological conditions most conducive to rapid frost deposition included clear skies, a shallow layer of moist air in contact with the surface, high water-vapor content in that layer, a gentle but consistent breeze, recent cold weather, short day-length, and wind direction. However, the main emphasis in this frost analysis is on surface and near surface meteorological factors that influence frost deposition. Three conditions must exist for

Table 8. Conditions for frost deposition.

1) The pavement temperature (T_P) must be at or below the melting point. ($T_P \leq 273.16$ K)
2) The pavement temperature (T_P) must be less than the 2-m dew point temperature (T_D) and the 2-m air temperature (T_A). ($T_A \geq T_D > T_P$)
3) The 2-m dew point temperature (T_D) must be near 273.16 K or well above the pavement temperature (T_P) for a period of time.

frost deposition (Takle, 1990) which are described in Table 8. The first condition ensures that when the pavement temperature is at or below the melting point, any moisture deposited will be in the form of frost rather than liquid (dew). The second condition ensures that the moisture available in that 2-m layer has a downward flux onto the pavement surface. The third condition suggests that greater differences between the pavement and dew point temperature lead to substantial amounts of frost deposition. In addition, when the deposition period is long, a significant amount of frost may accumulate on the pavement surface, possibly sufficient to cause slippery conditions.

The frost accumulation model (FAM2000) described in Section 4.4 uses the three basic conditions in Table 8 as well as wind speed to estimate frost formation. Moderate wind speeds at 5-m provide low-level wind shear to promote water-vapor diffusion toward the surface through turbulent processes. A linear relationship between the wind speed and frost deposition is assumed and used in the frost model. Figure 4 illustrates RWIS meteorological and pavement temperatures (based on the criteria outlined in Table 8) accompanying observed frost formation on a bridge deck near Mason City, Iowa on January 19, 1997.

4.3.3. Basic assumptions

Several factors can affect frost deposition. Salt solutions applied to the pavement surface act to inhibit frost formation as long as the solutions remain undiluted. Because the IaDOT does not record the times when salt is used or the amount of salt applied to pavement surfaces, this analysis assumes that no residual salt is present on the bridge decks analyzed. Thus, residual salt is not taken into account in the frost accumulation model. In addition, the frost model assumes that no snow or liquid water is present on the pavement surface to promote

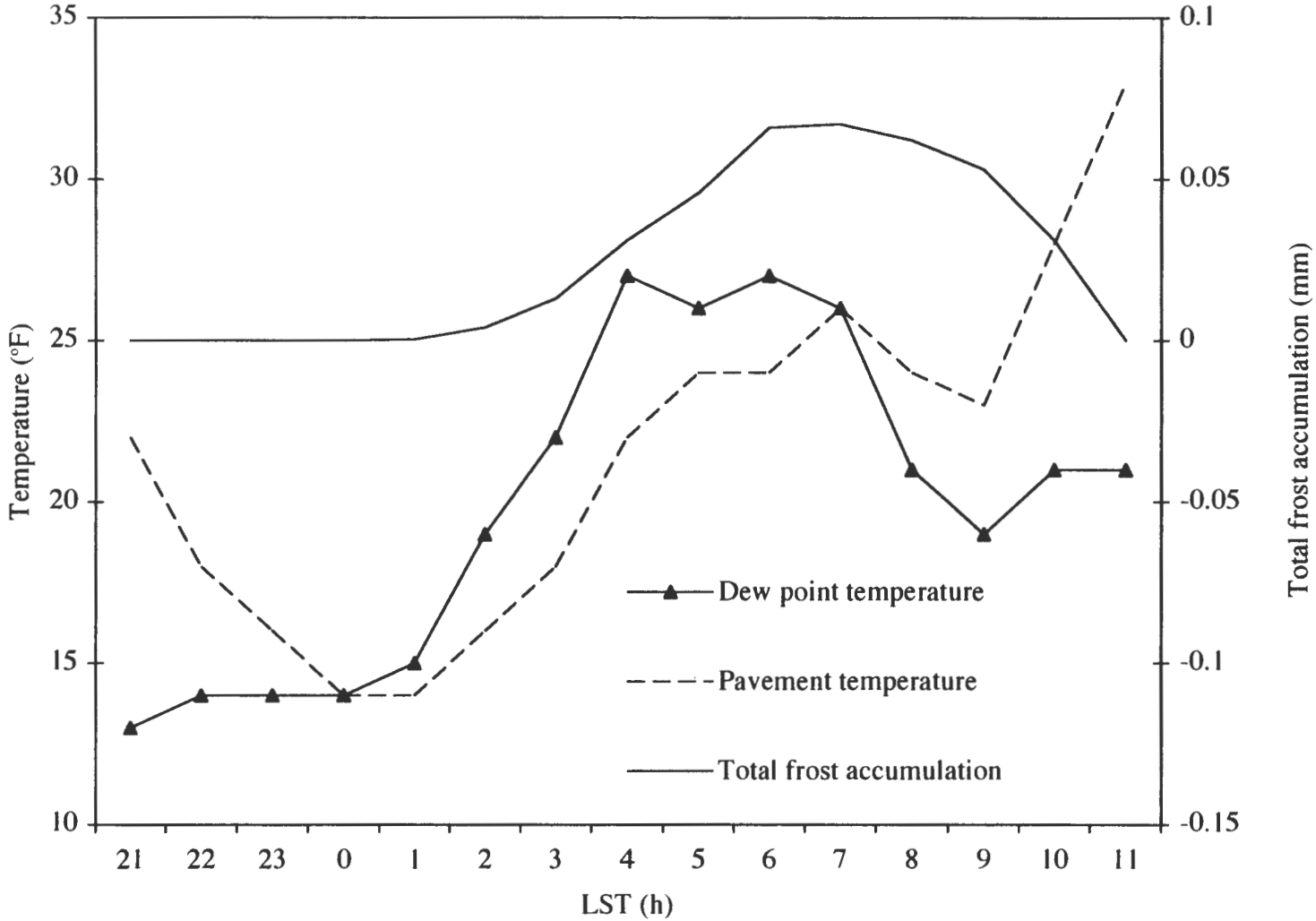

Figure 4. Conditions accompanying frost formation.

or suppress frost formation. This assumption may lead to the underestimation (snow) or overestimation (water) of deposited frost on roadways and bridge decks. The frost model also assumes that no precipitation has fallen immediately before or during frost deposition (which may underestimate accumulations) or after deposition (which may overestimate frost accumulation or melt any frost away before the maintenance personnel made their daily surveys). It is important to note that cases where the criteria for frost deposition (Table 8) were met and precipitation occurred during the deposition period were eliminated from this study. Only three cases met these conditions.

4.4. Frost accumulation model

The frost accumulation model (FAM2000) calculates the total depth of frost accumulated on bridge decks over time. The model uses the basic physics of pavement frost formation found in Section (4.3 b). Consequently, the model frost accumulation is essentially controlled by the bridge deck temperature, the moisture content of the air near the surface and the near surface wind speed.

The governing equation used within the model to represent the net flux of moisture, F_f, onto the pavement (Rayer, 1987; Barker and Davies, 1990; and Sass, 1992, 1997) is

$$F_f = \rho_d \overline{(w' q_s')}_s, \tag{1}$$

where ρ_d is the density of dry air, w′ represents the turbulent vertical velocity, and q_s' is the specific humidity with all variables being under saturated conditions at the surface. Using the transfer coefficient formulation to parameterize (1),

$$F_f = \rho_d C_E U(q_s(a) - q_s(g)) \tag{2}$$

where $q_s(a)$ is the specific humidity of air at 2-m and $q_s(g)$ is the specific humidity of air at the pavement surface. The transfer coefficient, $C_E = 10^{-3}$ (see Stull, 1988), is held constant due to the assumption that the stability of air is fixed. U is the 5-m RWIS wind speed (m s^{-1}). By use of Dalton's Law of partial pressures ($p = e + p_d$) and the ideal gas law, equation (2) becomes

$$F_f = \varepsilon R_d^{-1} C_E U(e - e_S(T_P)) T_A^{-1} \tag{3}$$

which is similar to that used in Hewson and Gait (1992) where e is the actual vapor pressure at 2-m, $e_S(T_P)$ is the saturation vapor pressure of the surface pavement temperature, and T_A is the 2-m RWIS air temperature. R_d is the gas constant for dry air with units of $J\,kg^{-1}\,K^{-1}$, and ε is the ratio of molecular weights between water and dry air. All temperatures have units of Kelvins. The difference in saturation vapor pressures, D, between the atmosphere and the pavement surface is calculated by use of the Clausius-Clapeyron equation,

$$D = e_S(T_O)\{\exp[L_D/R_V(T_O^{-1} - T_D^{-1})] - \exp[L_D/R_V(T_O^{-1} - T_P^{-1})]\} \quad (4)$$

where L_D is the latent heat of deposition at the freezing point with units of $J\,kg^{-1}$. R_V is the gas constant for water vapor with units of $J\,kg^{-1}\,K^{-1}$, and $e_S(T_O)$ is the saturation vapor pressure at T_O = 273.16 K with units of Pascals. To allow for weak deposition when conditions are just saturated ($T_D = T_P$) a small adjustment to the 2-m RWIS dew point temperature is performed,

$$T_D = T_P + 0.1. \quad (5)$$

The rate of growth in depth of frost as a function of time (in $m\,s^{-1}$) can be expressed as

$$R(t) = \rho_f^{-1}\varepsilon R_d^{-1} C_E U D T_A^{-1}, \quad (6)$$

after equation (3) is divided by a constant density of frost ($\rho_f = 0.1\ g\ cm^{-3}$). The complete derivation of equation (6) is given in Appendix A. Melting of frost is determined from the snow melt equation (SME) in NCEP's Eta model for $T_P > 273.16$ K, where the melt (SME) is

$$SME = (-10E(T_P - 273.16)(T_P^4 F + 1)T_P^{-1}). \quad (7)$$

SME has units of $m\,s^{-1}$, and $E = 1.0513 \times 10^{-8}\ m\,s^{-1}$ and $F = 6.48 \times 10^{-8}\ K^{-4}$ are constants in the melting equation. Equations (6) and (7) are multiplied by 1000 mm m^{-1} and 60 s min^{-1} to get rates with final units in mm min^{-1}. The model allows for a downward net flux of moisture (deposition) onto the pavement surface (A), an upward net flux of moisture (evaporation or sublimation) from the pavement surface (B), melting of frost with no deposition of moisture allowed on the pavement surface (C), and melting as well as evaporation or sublimation of frost at the same time from the pavement surface (D). The growth rate of frost, R(t), can be summarized in equations (8).

$$R(t) = \left\{ \begin{array}{l} (A) \Rightarrow \left[\text{if } T_p \leq 273.16 \text{ K and } D > 0 \text{ then } R(t) > 0 \right] \\ (B) \Rightarrow \left[\text{if } T_p \leq 273.16 \text{ K and } D < 0 \text{ then } R(t) < 0 \right] \\ (C) \Rightarrow \left[\text{if } T_p > 273.16 \text{ K where } R(t) = \text{SME (8) then } R(t) < 0 \right] \\ (D) \Rightarrow \left[\text{if } T_p > 273.16 \text{ K and } D < 0 \text{ then } R(t) < 0 \right] \end{array} \right\} \quad (8)$$

The time interval between the calculations, Δt, is one minute. Finally, total frost depth (TFD) is the aggregate of incremental increases and decreases in frost depth as long as the sum is not negative (9),

$$TFD = \sum R(t)\, \Delta t. \quad (9)$$

The source code for FAM2000 is given in Appendix B.

4.5. Model results

RWIS data gathered from the five RWIS sites were used as input for several frost model runs. For the 462 frost observations, the model produced 88 cases of positive frost accumulations (Appendix C), ranging from a low of 10^{-5} mm to the largest value of approximately 0.07 mm. For those cases, highway maintenance personnel observed frost on pavement surfaces 42 times (hits) and did not observe frost 46 times (false alarms). In addition, 6 events occurred where no frost was calculated by the model, but maintenance personnel observed frost on pavement surfaces (misses). Finally, the remaining 368 observations (correct negative prediction), in which the model produced no frost accumulations, were associated with the absence of frost observed by IaDOT winter maintenance personnel.

A thorough review was completed to find the reason behind the 6 missed events. All the missed events occurred between December 1995 and January 1996 in Waterloo. RWIS data in Waterloo and surrounding locations showed that the 2-m dew point temperature and the 2-m air temperature was less than the pavement temperature generally under overcast conditions. In addition, the data from the Waterloo RWIS site correlated well with adjacent site data. Consequently, the model did not produce any frost accumulation. The review indicated that

bridge deck frost would not have been caused from radiation cooling effects or warm air advection processes. Other than the possibility of human error, recent snows and overnight re-freezing conditions may have been the cause of the frost observations.

From this we conclude there may be a systematic discrepancy between modeled and observed frost for the Waterloo site for this 2-month period. Resolution of this discrepancy could very well increase accuracy of the model beyond the level discussed in the following sections.

4.6. Binary contingency table methodology, results and discussion

4.6.1. Methodology

A binary contingency table approach is used to compare the results of forecasted frost accumulations to the human frost observations (Table 9). The model frost predictions were

Table 9. Binary contingency table.

		Human Observations	
		Y	N
Forecast	Y	A Hits	B False Alarms
	N	C Misses	D Correct Negative Prediction

used to calculate probability of detection (also commonly known as "hit rate") and a false alarm rate. Previous studies have agreed on the definition of probability of detection (POD) or hit rate (H),

$$H = A/(A + C). \tag{10}$$

However, there is disagreement on the equation used to calculate the false alarm rate (FAR). For example, the form of the FAR equation (11) found in Wilks (1995) is

$$FAR1 = B/(A + B), \tag{11}$$

while another form of the FAR equation (12) is given by Mason (1982), Swets (1988),

$$FAR2 = B/(B + D) \tag{12}$$

and Takle (1990).

Marzban (1998) used a binary contingency table approach to define a "rare-event situation" while applying the equation from Wilks (1995). A rare-event situation is determined when D >> B, the number of misses is on the same order of magnitude as the number of hits (C ~ A), and $N_0 = (B + D) >> N_1 = (A + C)$. It is important to note that the value of D would increase significantly while the other factors (A, B, and C) would probably remain unaffected if warm season frost calculations were added into the contingency. Also, C will approach or equal the order of magnitude of A as more cold season events are analyzed. Using the cold season results from Table 9 and the technique from Marzban, the formation of frost on bridges is classified as a rare-event situation. Therefore I choose equation (11) as being most applicable to frost analysis, although both forms are calculated for comparison.

4.6.2. Results

The values of the hit rate, H = 0.875, and the false alarm rates, FAR1 = 0.523 and FAR2 = 0.111, suggest that the model did detect frost events well based on the information outlined in Table 9.

The frequency distribution of (the log of) frost depths (Figure 5) reveals a bimodal pattern with most likely depths being between 0.002 mm and 0.017 mm. Both curves were tested for normality. The curve that represents the predicted model depths where observed frost (hits) was determined to be non-normally distributed with a skewness toward larger calculated accumulations. However, the positive frost accumulations in which IaDOT personnel did not observe frost (false alarms) were approximately normally distributed. The Wilcoxen Rank Sum hypothesis test was used to determine if the two separate curves have significantly different population means even if the curves are not necessarily normally distributed. The null hypothesis (that the two curves have the same population mean) failed, thus, indicating that the two population means are significantly different confirming that the frost model FAM2000 is capable, in a statistically significant sense, of distinguishing frost occurrences from the non-

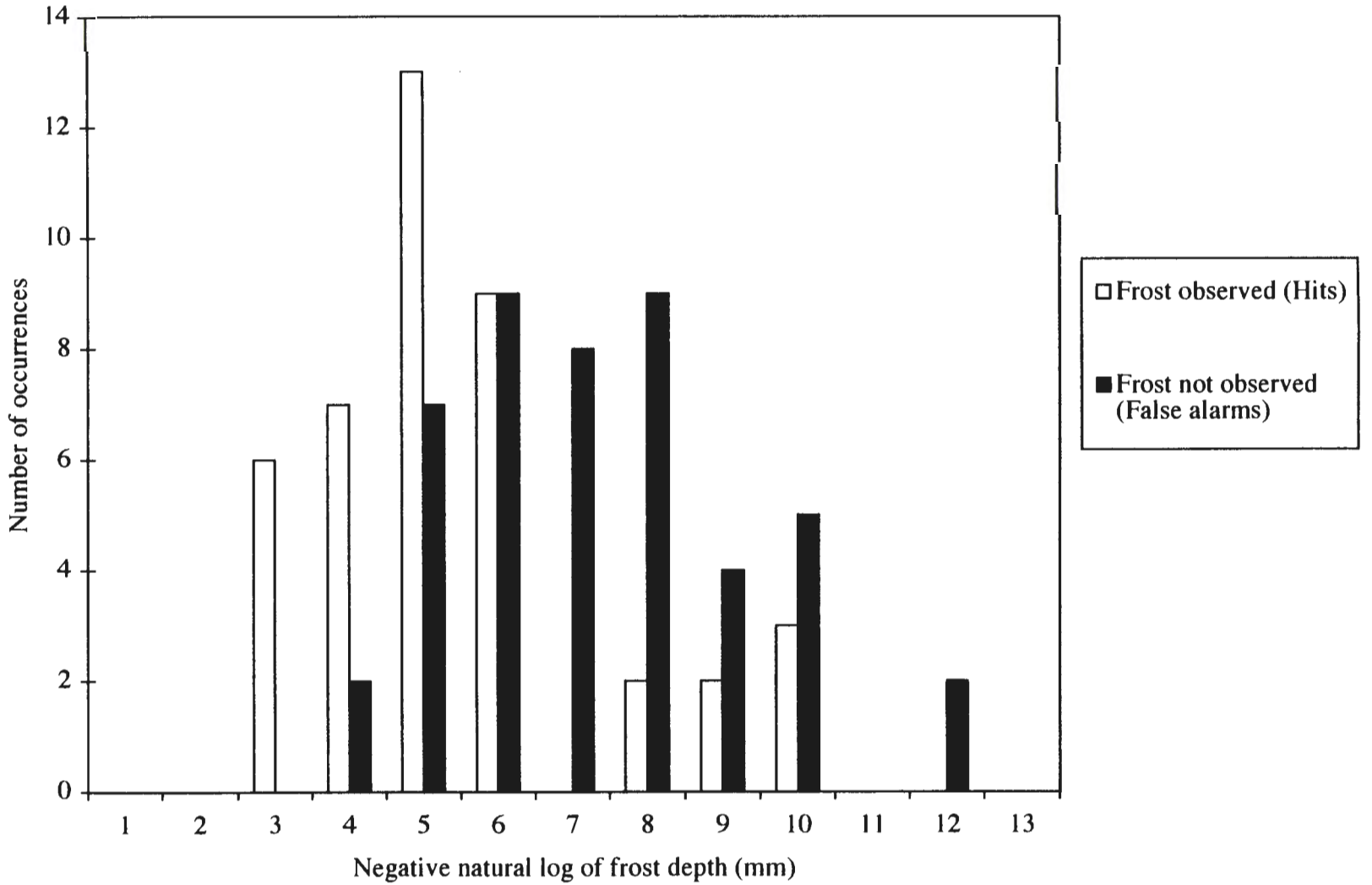

Figure 5. Frequency distribution of (the log of) frost depths.

occurrences.

A minimum (greater than zero) frost accumulation is required to be visible by humans. By moving the threshold value for observable frost from 0 mm (as used in Table 9) to higher values, the false alarm rate improves as the hit rate degrades. Regardless of the threshold used, FAR1 gives higher false alarm rates than FAR2. Table 10 and Table 11 show the computed rates for the various thresholds. Appendix D gives the contingency table adjustments for the various threshold frost depths. In Figure 6 are plotted the hit and false alarm rates for bridges for various values of model threshold frost depths using both forms of the false alarm rate equations.

The general trend in Figure 6 is for both hit and false alarm rates to decrease as the threshold depth increases. The best choice of threshold was defined to be the value that best discriminates between frost and no frost, i.e. the greatest difference between hit rate and false alarm rate (ΔR = hit rate – false alarm rate). When computing false alarm rates using FAR1, the best result, $\Delta R = 0.389$, occurred with the threshold depth of 0.002 mm. However when using FAR2, the best result, $\Delta R = 0.769$, occurred with a much lower threshold of 10^{-5} mm.

4.6.3. Discussion

When no frost was observed by maintenance personnel but TFD > 0 (false alarms), the predicted depths tended to be on the lower end of the range of calculated accumulations and cases where frost was observed, and TFD > 0 (hits) mostly occurred for the higher end of the range of accumulations. This suggests that the low values of frost accumulation may correspond to events for which frost may be accumulating but not to a depth observable by IaDOT procedures.

The stated goal is to correctly forecast all real frost events and limit the number of false alarm events. Additional work, not presented in this study, has shown that an adjustment to the 2-m dew point in the original frost model based on meteorological principles reduced false alarms while correct forecasts were unaffected (Nichols, 1999). However, further testing is

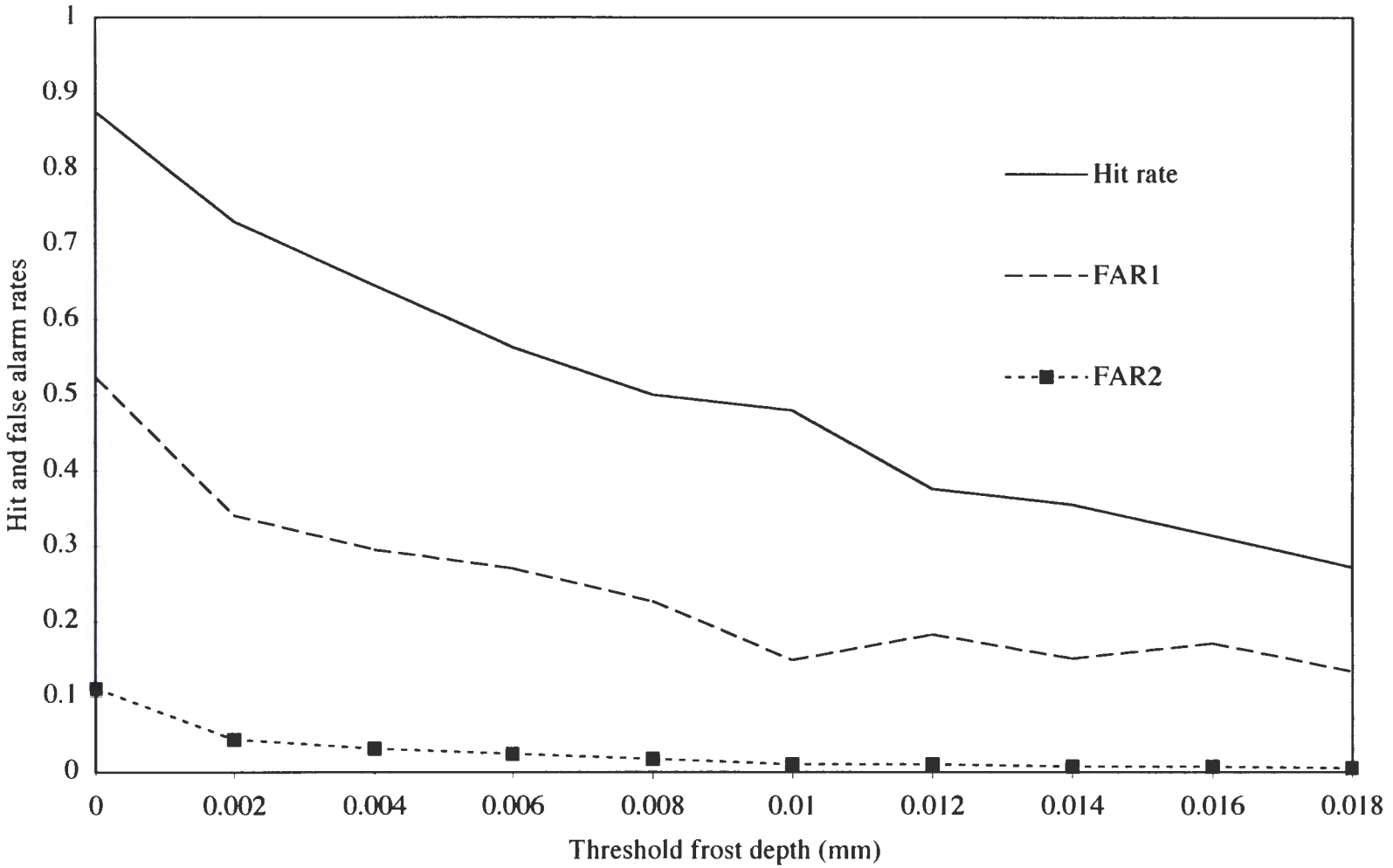

Figure 6. Effect on H and FAR of various thresholds.

Table 10. SDT calculations with FAR1.

Threshold depth (mm)	Hit rate (H)	False alarm rate (FAR1)	ΔR (H-FAR1)	Decision criterion (X_c)	Index of accuracy (d′)	Criterion placement (β)
0	0.875	0.523	0.352	-0.06	1.09	0.48
10^{-5}	0.875	0.512	0.363	-0.03	1.12	0.52
10^{-4}	0.813	0.500	0.313	0.00	0.89	0.67
0.000335	0.771	0.486	0.285	0.035	0.78	0.76
10^{-3}	0.729	0.426	0.303	0.19	0.80	0.85
0.002	0.729	0.340	0.389	0.41	1.02	0.90
0.007	0.542	0.257	0.285	0.65	0.76	1.23
0.018	0.271	0.133	0.138	1.11	0.50	1.54
			AVG	0.29	0.87	0.87

Table 11. SDT calculations with FAR2.

Threshold depth (mm)	Hit rate (H)	False alarm rate (FAR2)	ΔR (H-FAR2)	Decision criterion (X_c)	Index of accuracy (d′)	Criterion placement (β)
0	0.875	0.111	0.764	1.22	2.37	1.08
10^{-5}	0.875	0.106	0.769	1.25	2.40	1.13
10^{-4}	0.813	0.094	0.719	1.32	2.21	1.61
0.000335	0.771	0.085	0.686	1.37	2.11	1.94
10^{-3}	0.729	0.063	0.667	1.53	2.14	2.68
0.002	0.729	0.043	0.686	1.72	2.14	4.02
0.007	0.542	0.022	0.520	2.01	2.12	7.49
0.018	0.271	0.005	0.266	2.57	1.96	22.56
			AVG	1.62	2.18	5.31

needed to conclusively evaluate this preliminary model improvement. Also other adjustments to IaDOT winter procedures could act to improve the quality and accuracy of model verification, such as, if IaDOT personnel recorded the exact time of frost observance, recorded the amount of chemical solution used to suppress frost accumulation, and increased the time period in the morning they look for frost deposition.

4.7. Forecast accuracy and decision criterion

4.7.1. Signal detection theory

Signal detection theory (SDT), outlined in Mason (1982a), is a technique used to separate forecast accuracy from the decision criterion. Essentially, SDT is an extension of probabilistic forecasting using binary contingency table methodology. The SDT technique has been applied to forecasts of a variety of weather variables (Mason, 1982b; McCoy, 1986; Takle, 1990 and Buizza et al., 1999). SDT is used in this frost analysis in which the probabilistic forecast is a set of contingency tables where the hit and false alarm rates were computed based on different threshold frost depths.

The SDT technique, described by Green and Swets (1974) and Swets (1973, 1986, 1988), allows for computations of indices d' and β. The basic SDT index of accuracy, d', is defined as the number of standard deviations separating the means of the (assumed normal) distributions of decision criterion preceding occurrence (hits) and preceding non-occurrence (false alarms). Thus, if the probabilities of the hit rate and false alarm rate are equal, $d' = 0$ which indicates no skill. Higher values of d' indicate greater skill. The criterion placement, β, is the likelihood ratio that measures the occurrence against the non-occurrence. A high criterion placement value ($\beta > 1$) ensures a low false alarm rate at the expense of a lower hit rate. A low criterion placement value ($\beta < 1$) suggests a bias toward maintaining a high hit rate at the expense of a higher false alarm rate, and a value of $\beta = 1$ shows no bias towards the hit or false alarm rate. Table 12 defines the terms used to compute SDT values.

Table 12. Signal detection theory (SDT) definitions.

decision criterion = $x_c = P^{-1} (1 - F)$

index of accuracy = $d' = x_c - P^{-1} (1 - H)$

criterion placement = $\beta = \exp \{ - 0.5 [d' (d' - 2x_c)]\}$

P^{-1} = inverse of normal probability distribution function.

4.7.2. Relative operating characteristic curves

By taking bridge values from Table 10 and 11, a set of point estimates can be plotted on a hit rate/false alarm rate graph. These points define a SDT curve called the relative operating characteristic (ROC) generated from normal distributions (Mason, 1982a; Swets, 1986). The range of threshold frost depths observed in our study does not span the entire range of hit and false alarm rates, but the limit cases must tend toward the points (0,0) and (1,1). Figure 7 is a curve of hit rates and false alarm rates (FAR1) for various frost depths. A comparable plot for the same range of threshold frost depths but using the other form of the false alarm rate equation (FAR2) is shown in Figure 8.

The goal of using the ROC curves is to find an "optimum" combination of hits and false alarms and to quantify the impact of lowering FAR or raising H. Results from Figure 7 and Table 10 show that the optimum combination of high accuracy and large criterion placement is for the threshold frost depth at 0.002 mm where $d' = 1.02$ and $\beta = 0.90$. The best results for FAR2 (Figure 8 and Table 11) are found for the same threshold frost depth (0.002 mm) where $d' = 2.14$ and $\beta = 4.02$, which indicates a higher accuracy with a strong bias toward minimizing false alarms.

4.7.3. Area under the ROC curves

Following Swets (1988), another measure of accuracy is defined as the area (A) under the ROC curve. If A = 1, the probabilistic forecast system is considered perfect, with accuracy decreasing with decreasing A. A = 0.5 gives a useless forecast system. More specifically a

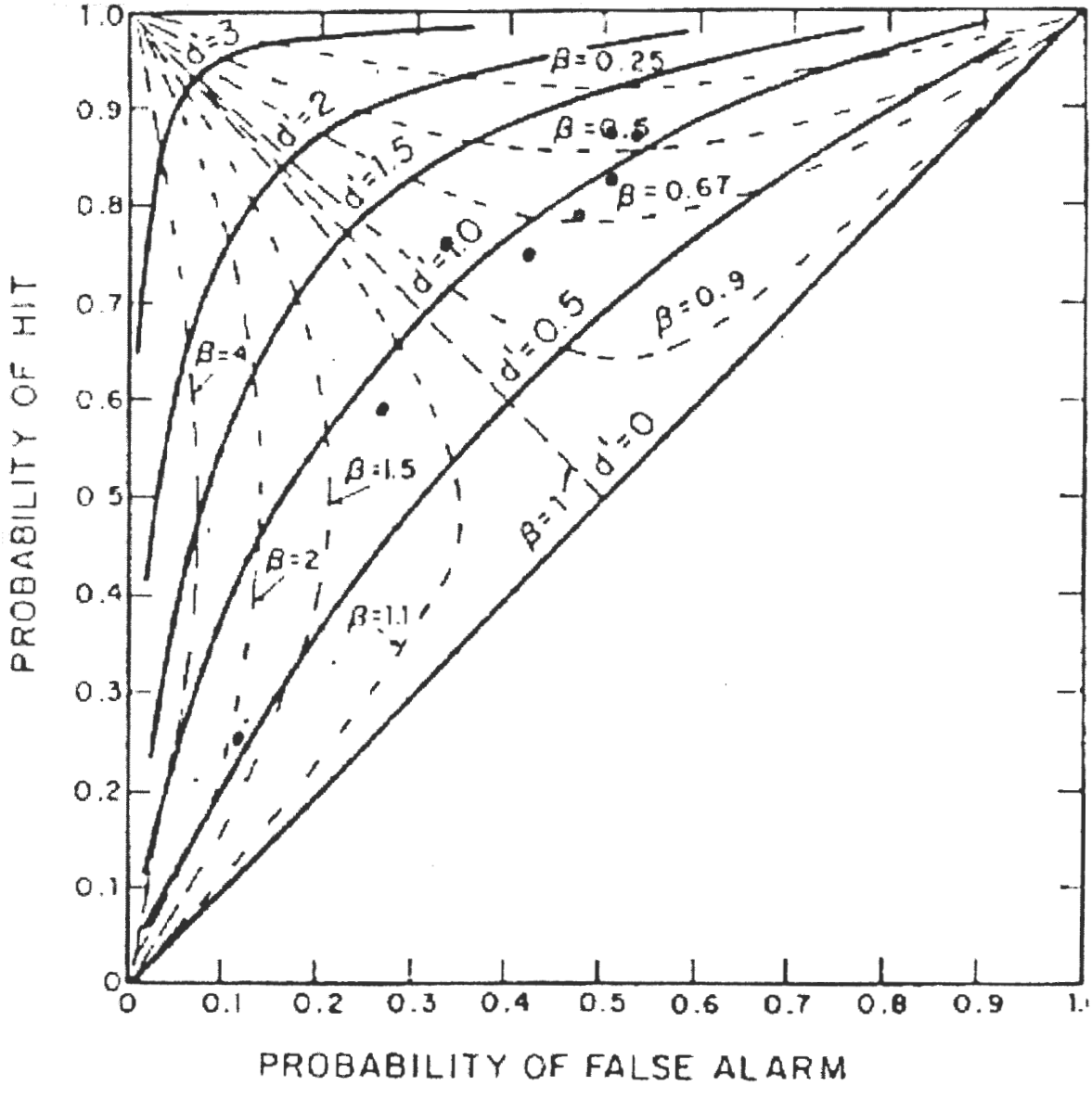

Figure 7. The set of black dots defines the ROC curve using point estimates of H and FAR1 for the various threshold frost depths.

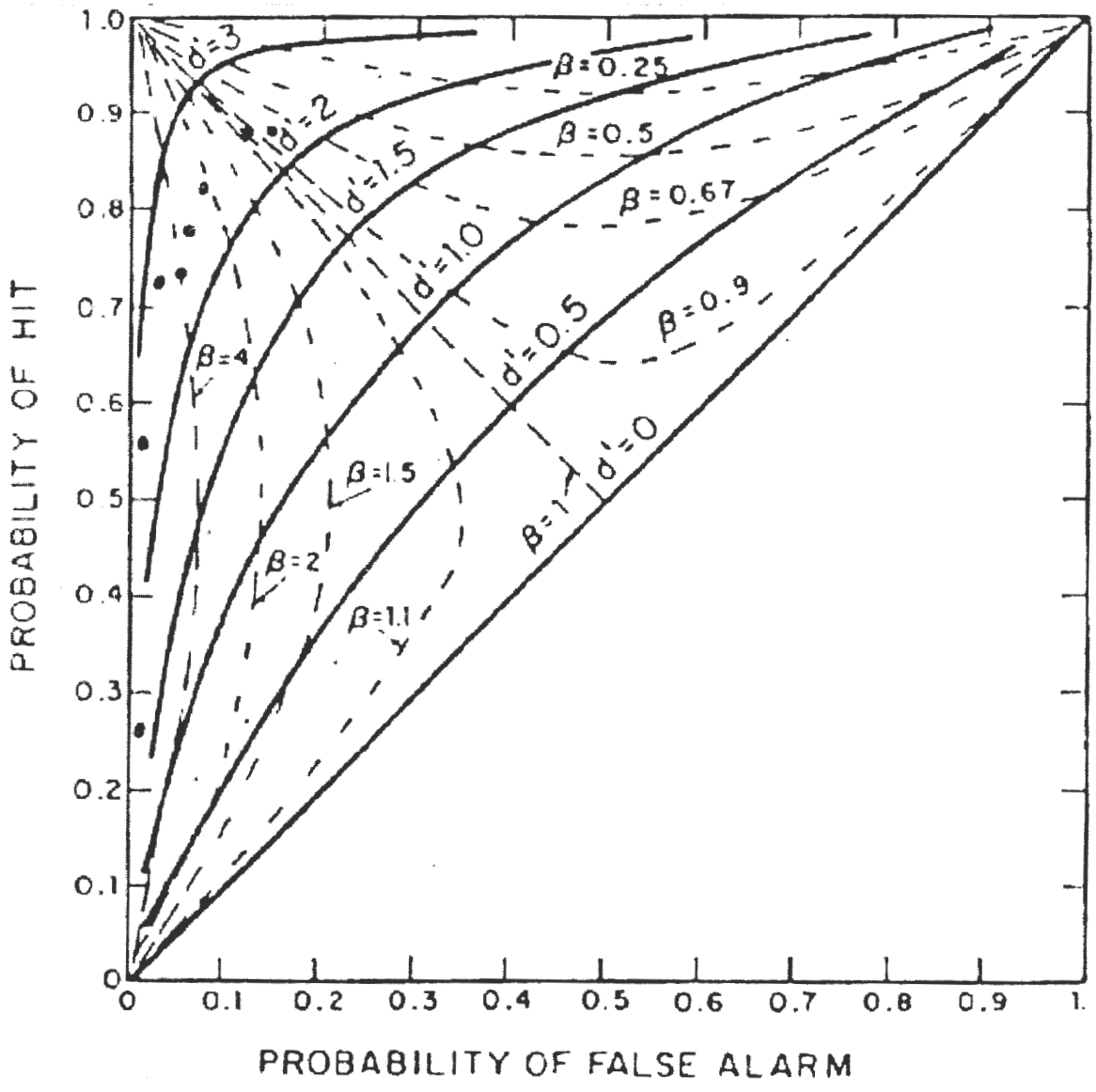

Figure 8. The set of black dots defines the ROC curve using point estimates of H and FAR2 for the various threshold frost depths.

a perfect forecast system has a 100% hit rate and 0% false alarm rate (A = 1), while a useless system has a ROC curve that coincides with the diagonal (d′ = 0) on the ROC curve and an area under the curve A = 0.50. Swets suggests that A values less than 0.70 lead to insufficient accuracy in the forecast system to provide much practical value, and values between 0.70 and 0.90 define sufficient accuracy in the system. However, a few texts warn of the use of arbitrary threshold values to define system accuracy (Buizza et al., 2000; Juras, 2000; Wilson, 2000) using the area under the ROC curve. For example, Juras (2000) argues that the limit value for A should vary and depend on the variability of climatological frequencies of an event within a homogeneous region.

Integration of the area under the ROC curve given in Figure 7 for bridges yields a value A = 0.71 and from Figure 8 A = 0.91. Thus, using the qualitative threshold criterion range (0.70 – 0.90) from Swets, the frost model (FAM2000) has potential practical value. Even though the A value of forecasts made with the frost model may be reduced by the uncertainty in the input data, FAM2000 has the potential to be skillful. Also, these results indicate that FAM2000 has slightly higher accuracy than the expert system used in Takle (1990).

4.8. Logistic regression model

Logistic regression analysis is a well known statistical procedure commonly used in many scientific fields of study (Agresti, 1984; Freeman, 1987; Hosmer and Lemenshow, 1989). Here it is used to investigate the relationship between the binary response (frost observations) and the explanatory response (model frost depths) variables. Cox and Snell (1989) give a thorough discussion of binary response model methodology.

A simple linear logistic regression model (13) was used to describe the probability of a predicted frost depth being observed by IaDOT personnel given a particular calculation of frost depth by the model:

$$\log (p/(1 - p)) = \alpha + \beta \mathbf{x} \qquad (13)$$

Let **x** be the predicted frost depth (TFD in Eq. 10), and p be the probability of observed frost,

leaving (1 - p) as the response probability frost was not observed. By use of maximum likelihood analysis (Aitchison and Silvey, 1957 and Ashord, 1959), the intercept estimate, α, was calculated to be -3.0575, and the slope estimate, β, was 296.9. Solving for p gives

$$p = (1 + e^{-(\alpha + \beta x)})^{-1}. \quad (14)$$

If forecast values of air temperature, dew point temperature, pavement temperature, and wind speed are used to drive the frost accumulation model to provide **x** (= TFD) then (14) gives the probability that an IaDOT employee will see frost under the predicted conditions.

Figure 9 shows the logistic regression curve for the probability of observing frost (p) for various values of predicted frost depths (**x** = TFD). The general trend in Figure 9 is for p to increase as the depth increases. Results in Figure 9 show that when p = 1 (≤ 0.1), $\mathbf{x} \geq \sim 0.03$ mm (≤ 0.003 mm) and show that the minimum threshold frost depth to be observed by a human within a maintenance vehicle is approximately 0.01 mm (p = 0.50), which is at the upper end of the range (0.002 – 0.01 mm) of observable depths suggested by Hewson and Gait (1992). Therefore frost depths less than 0.01 mm are less likely to be observed by IaDOT maintenance personnel than those exceeding 0.01 mm. Also, under extreme frost deposition, total frost depths equal to or greater than 0.03 mm (p = 1) are more likely to be observed by IaDOT maintenance personnel.

4.9. Summary

A model (FAM2000) based on simple concepts of moisture flux to the surface has been developed based on current and forecasted RWIS air temperatures, dew point temperatures, pavement surface temperatures, and wind speed. The model uses the RWIS data to calculate expected amounts of accumulated frost (TFD) on bridges. Bridge deck frost was shown to arguably be a rare-event situation; therefore, forecast skill of the model was evaluated using the false alarm rate (12) appropriate for rare events. Results from the SDT and ROC analyses suggest that the prediction of frost on bridge decks by use of the model has sufficient accuracy to be used as an operational tool; however, uncertainty of input information (i.e. forecast RWIS

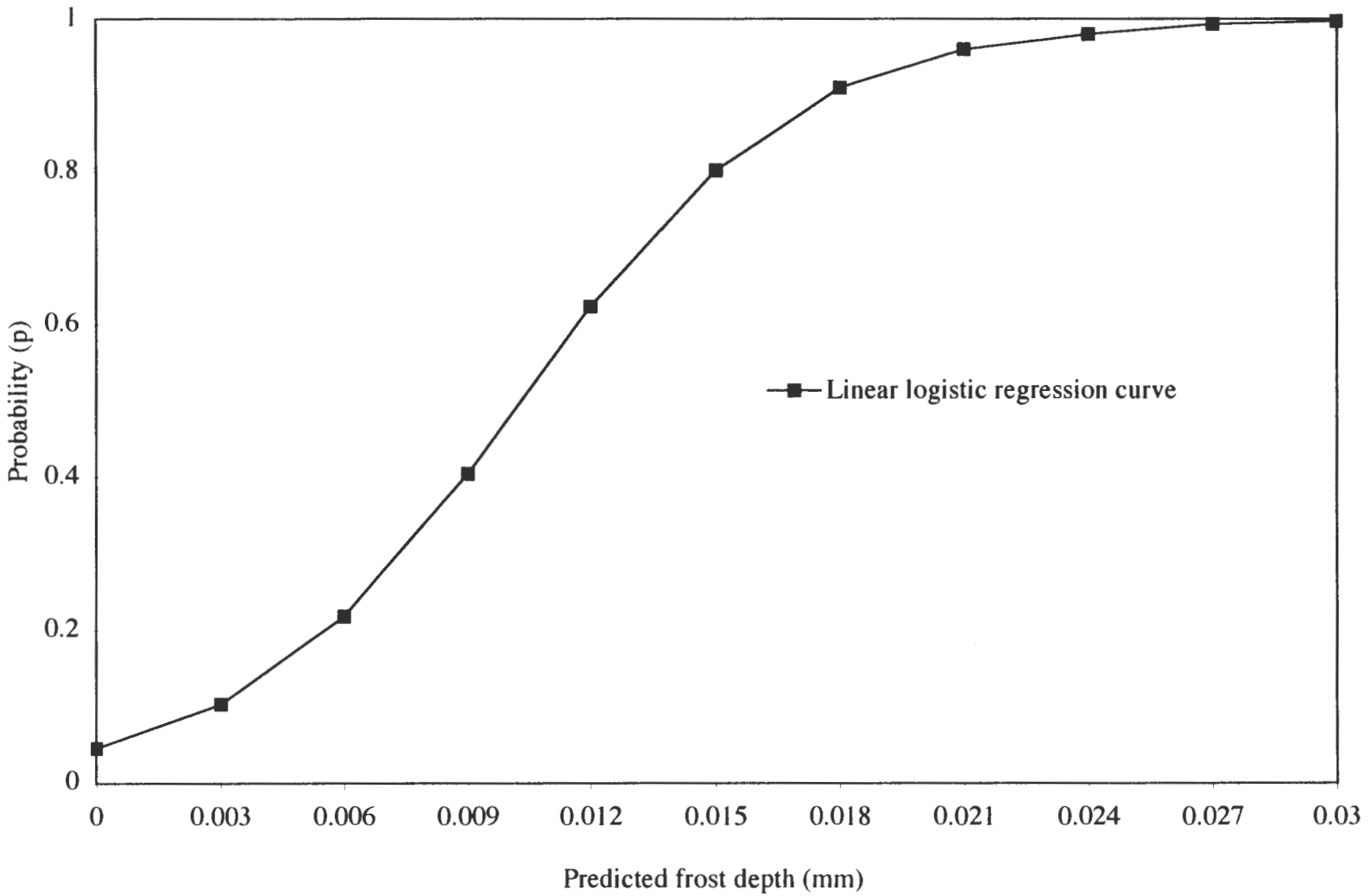

Figure 9. The probability (p) that IaDOT personnel will see frost for a predicted frost depth.

values) will correspondingly degrade the prediction of frost accumulation.

A key parameter determined was the threshold accumulated frost depth calculated by the model that corresponds to the minimum observable frost seen by IaDOT maintenance personnel from inside a moving vehicle while making surveys of bridges. A logistical regression technique was used to determine the probability (p) that a maintenance worker will observe frost for a given calculated frost depth (TFD). Results indicated that a threshold depth of around 0.01 mm seems to be the minimal likely amount of frost accumulated on a bridge deck that is observable under IaDOT procedures.

Finally, some assumptions used in the simple model (e.g., use of neutral drag coefficient) and its application to an elevated surface (e.g., elevated bridge deck as opposed to a flat surface of infinite horizontal extent at the ground) might introduce biases into the model. Limitations of observations (e.g., frost occurring after observer has completed his/her observation, frost not forming due to residual frost-suppressing chemical) also may reduce accuracy of the model. A systematic comparison of model calculations with observations would allow evaluation of model accuracy and suggest ways of tuning for improvement.

CHAPTER 5. CONCLUSIONS

This study examined the use of RWIS data in the fight against nocturnal slippery road conditions during the cold season for site-specific locations in the state of Iowa. The study centered around the development of a few forecast procedures based on simple physical concepts about the prediction of pavement temperature cooling and moisture deposition in the form of frost on bridge decks.

The pavement temperature analysis (Chapter 3) concentrated on the meteorological effects of RST cooling due to cloud cover and seasonal effects. Urban and rural RST cooling trends offer roadway maintenance personnel guidance for treating roadways and bridges for frost, snow, and ice conditions as well as supplementing pavement temperature forecasts. For example, maintenance personnel can compare the calculated cooling rate trends for bridges and roadways to pavement temperature forecasts provided to them by their private weather forecasting source. This comparison could lead to a refinement on the timing of onset of freezing conditions at specific RWIS locations. In general, the calculated cooling rates and mean urban lag times can be used as a tool in combination with other forecast products to determine expected pavement cooling for Des Moines and Cedar Rapids. Cooling trends were not always the same, so it is important to note that pavement temperature cooling trends for one city can not necessarily be applied to another city.

The frost analysis (Chapter 4) focused on the prediction of frost on bridge decks based on RWIS temperature and wind speed data from five Iowa sites. When maintenance personnel are faced with the threat of nocturnal frost formation, they factor non-meteorological as well as meteorological information into their prevention plans. When considering all information available, IaDOT management can use the SDT procedure to determine the optimum combination of hit rate and false alarm rate based on the established threshold frost depths. For example, when they receive a forecast frost accumulation, management can use the SDT procedure to evaluate the forecast accuracy in combination with available non-meteorological

information (i.e. residual salt residue on pavement surfaces, traffic volume, or environmental issues). In addition, management can compare the results of logistic regression probability of a forecasted maximum frost depth to internal frost prevention standards within the IaDOT.

This study offers forecast procedures to aid in the prediction of slippery road conditions across Iowa during the cold season. The procedures developed concerning pavement temperature cooling and frost formation give management personnel tools to help manage and forecasters tools to help forecast frost events.

APPENDIX A. DERIVATION OF FROST ACCUMULATION MODEL

Net flux of moisture onto the pavement:

$F_f = \rho_d \overline{(w'q_s')}_s$

$\rho_d \Rightarrow$ density of dry air

$w' \Rightarrow$ turbulent vertical velocity

$q' \Rightarrow$ specific humidity

$(\quad)_s \Rightarrow$ indicates saturation at surface

Parameterization by use of transfer coefficient formulation:

$F_f \Rightarrow \rho_d C_E U (q_s(a) - q_s(g))$

$C_E \Rightarrow$ transfer coefficient

$q_s(a) \Rightarrow$ specific humidity of air at 2-m

$q_s(g) \Rightarrow$ specific humidity of air at pavement surface

$U \Rightarrow$ 5-m wind speed

Hint:

Units of F_f are (mass)(area x time)$^{-1} \Rightarrow gcm^{-2}s^{-1}$

Use Dalton law of partial pressures and ideal gas law:

$\varepsilon = 0.622$

$p \Rightarrow$ atmospheric surface pressure

$$e = e_s(T_o)\exp\{ L_d R_v^{-1} ((T_o^{-1}) - (T_p^{-1}))\}$$

$e \Rightarrow$ saturation vapor pressure at 2-m

$$q_s(a) = \varepsilon e p^{-1} \Rightarrow \varepsilon p^{-1} e_s(T_o)\exp\{ L_d R_v^{-1} ((T_o^{-1}) - (T_d^{-1}))\}$$

$$e_s(T_p) = e_s(T_o)\exp\{ L_d R_v^{-1} ((T_o^{-1}) - (T_p^{-1}))\}$$

$e_s(T_p) \Rightarrow$ saturation vapor pressure at the pavement surface, T_p

$$q_s(g) = \varepsilon e_s(T_p) p^{-1} \Rightarrow \varepsilon p^{-1} e_s(T_o)\exp\{ L_d R_v^{-1} ((T_o^{-1}) - (T_p^{-1}))\}$$

$T_o \Rightarrow$ freeze point = 273.16 K

$e_s(T_o) \Rightarrow$ saturation vapor pressure at freeze point = 6.108 mb

$L_d \Rightarrow$ latent heat of deposition

$R_v \Rightarrow$ the specific gas constant for water vapor

Let:

$$F_f = C_E U ([\varepsilon p^{-1} e_s(T_o)\exp\{ L_d R_v^{-1} ((T_o^{-1}) - (T_d^{-1}))\}] - [\varepsilon p^{-1} e_s(T_o)\exp\{ L_d R_v^{-1} ((T_o^{-1}) - (T_p^{-1}))\}])$$

$$F_f = C_E U \varepsilon p^{-1} e_s(T_o) ([\exp\{ L_d R_v^{-1} ((T_o^{-1}) - (T_d^{-1}))\}] - [\exp\{ L_d R_v^{-1} ((T_o^{-1}) - (T_p^{-1}))\}]) T_a^{-1}$$

Substitution:

let $D = e_s(T_o)([\exp\{ L_d R_v^{-1} ((T_o^{-1}) - (T_d^{-1}))\}] - [\exp\{ L_d R_v^{-1} ((T_o^{-1}) - (T_p^{-1}))\}])$

To get growth in depth of frost with time, divide F_f ($gcm^{-2}s^{-1}$) by the density of frost.

Assume density of frost:
$\rho_f \Rightarrow 0.1$ x density of ice, $\rho_i = 1.0\ (gcm^{-3})$
$\rho_f \Rightarrow 0.1 \times \rho_i = 0.1\ (gcm^{-3})$

Rate of growth of frost with time:
$R(t) \Rightarrow F_f \rho_f^{-1} = \rho_f^{-1} C_E U \varepsilon R_d^{-1} D T_a^{-1}$

Simplify:
$R(t) = \rho_f^{-1} \varepsilon R_d^{-1} C_E U D T_a^{-1}$

R(t) is the governing equation to determine the frost accumulation rate.

APPENDIX B. FROST ACCUMULATION MODEL (FAM2000) SOURCE CODE

```
!
! FROST ACCUMULATION MODEL (FAM2000)
!
! PROGRAM DISCUSSION
!
! THIS IS A FORTRAN 90 DRIVER PROGRAM. THIS PROGRAM WAS CREATED
! AND MAINTAINED BY DAVID KNOLLHOFF. CREATION DATE (AUGUST 2000).
! THIS PROGRAM ACCEPTS DATA WITH A DATE AND TIME STAMP AS WELL AS
! 2-M AIR TEMPERATURE...2-M DEW POINT TEMPERATURE...5-M WIND SPEED
! AND PAVEMENT TEMPERATURE. THE PROGRAM QUALITY CONTROLS THE
! DATA STATING ANY ERRORS FOUND. THEN THE TIME/DATE STAMP IS
! CONVERTED INTO TOTAL MINUTES USING THE FUNCTION
! convert_date2min.f90. NEXT THE PROGRAM GOES THROUGH ANOTHER
! QUALITY CONTROL CHECK TO MAINTAIN CHRONOLOGICAL ORDER OF
! DATA. IF ERRORS ARE FOUND THE USER WILL BE NOTIFIED. THEN ONE
! MINUTE VALUES ARE CREATED USING A SUBROUTINE CALLED lin_inter.f90
! (LINEAR INTERPOLATION). AFTER THE LINEAR INTERPOLATION PROCESS
! HAS COMPLETED...THE PROGRAMS CALLS ANOTHER SUBROUTINE
! accumulation5.f90 TO CALCULATE (PREDICT) THE TOTAL DEPTH OF FROST
! ACCUMULATED FOR A BRIDGE DECK IN IOWA. FINALLY THE MINUTE
! VALUE OF THE DATE/TIME STAMP IS CONVERTED BACK INTO THE
! EQUIVALENT CALENDAR DATE AND TIME. THE DATA IS PRINTED TO THE
! SCREEN AND/OR A FILE NAMED output1.
!
! DEFINITIONS
!
! maxdim      = maximum number of lines allowed from calculations
! maxnum      = maximum number of lines allowed from input file
! yy          = 2 digit calendar year from input file
! mm          = 2 digit calendar month from input file
! dd          = 2 digit calendar day from input file
! hr          = 2 digit hour from archive file
! mtime       = the value in total minutes calculated using convert_date2min.f90 function
!               (minutes)
! savetime    = the stored old mtime
! ierrcnt     = number of errors from the chronological test
! dt          = the difference in time between consecutive observations (min)
! m           = loop counters for final data point
! i           = loop counters for initial data
! ict         = counter for final data point
! nvalues     = the number that represents the total number of lines in file
! aircnt      = number of errors in air temperature data
! dewcnt      = number of errors in dew point temperature data
! errorcnt    = total number of air in meteorological data
! speedcnt    = number of errors in wind speed data
! pavecnt     = number of errors in pavement temperature data
! assumecnt   = number of errors from meteorological assumptions
! air         = air temperature data (F)
! dew         = dew point temperature data (F)
! speed       = wind speed data (mph)
```

```
! pave          = pavement temperature data (F)
!  ar           = air temperature difference (F)
!  slopeair     = slope of air temperature over time (F/min)
!  dw           = dew point temperature difference (F)
!  slopedw      = slope of dew point temperature difference over time (F/min)
!  spd          = wind speed difference (mph)
!  slopespeed   = slope of wind speed over time (F/min)
!  p            = pavement temperature difference (F/min)
!  slopepave    = slope of pavement temperature (F/min)
!  prob         = probability of seeing a predicted frost depth (mm)
!
!  INITIALIZATION
!
   parameter (maxdim=90000)
   parameter (maxnum=10000)
   integer convert_date2min
   integer yy,mm,dd,hr,min
   integer yyy,mmm,ddd,hhh,mmin
   integer mtime(maxnum),savetime,ierrcnt,dt,newmin(maxdim)
   integer m,NN,MT,ict,aircnt,dewcnt,errorcnt,speedcnt,pavecnt
   integer assumecnt,I,nvalues
   real*8 air(maxnum),dew(maxnum),speed(maxnum),pave(maxnum)
   real*8 ar,slopeair,dw,slopedew,spd,slopespeed,p,slopepave
   real*8 TTA(maxdim),TTD(maxdim),WWS(maxdim),TTP(maxdim)
   real*8 AA,TA,SA,TDD,TD,SD,WSD,WS,SS,PP,TP,SP
   real*8 smr,R,Rsmr,depth,TFD,prob
   real*8 cela,Ka,celd,Kd,sped,celp,Kp,b,c,D,D1,D2
   character*80 filein
   aircnt=0
   dewcnt=0
   speedcnt=0
   pavecnt=0
   assumecnt=0
   errorcnt=0
   savetime=-1
   ierrcnt=0
   ict=0
!
!  FILE OF INTEREST
!
   print *,  'enter the name of your data array'
   read (5,fmt='(a80)') filein
   open (unit=200,file=filein,status='old')
   open (unit=201,file='output1',status='unknown')
   do i=1,maxnum
      read (200,100,end=9) yy,mm,dd,hr,min,air(i),dew(i),speed(i),pave(i)
100 format (2x,i2,1x,i2,1x,i2,3x,i2,1x,i2,4x,f10.2,1x,f10.2,1x,f10.0,1x,f10.2)
!
!  QUALITY CONTROL FOR METEOROLOGICAL ASSUMPTIONS
!
   if (air(i) .le. –50.d0 .or. air(i) .ge. 120.d0) then
    print *, yy,mm,dd,hr,min,air(i),'-- does not meet air temp assumption'
```

```
      aircnt=aircnt+1
                                                    endif
    if (dew(i) .le. –50.d0 .or. dew(i) .ge. 120.d0) then
     print *, yy,mm,dd,hr,min,dew(i),'-- does not meet dew temp assumption'
      dewcnt=dewcnt+1
                                                    endif
    if (speed(i) .lt. 0 .or. speed(i) .ge. 100) then
     print *, yy,mm,dd,hr,min,speed(i),'-- does not meet wind speed assumption'
      speedcnt=speedcnt+1
                                                  endif
    if (pave(i) .le. –50.d0 .or. pave(i) .ge. 120.d0) then
     print *, yy,mm,dd,hr,min,pave(i),'-- does not meet pavement temp assumption'
      pavecnt=pavecnt+1
                                                    endif
    if (dew(i) .gt. (air(i)+1.d0)) then
     print *, yy,mm,dd,hr,min,dew(i),air(i),'-- does not meet physical assumption'
      assumecnt=assumecnt+1
                                  endif
      errorcnt=aircnt+dewcnt+speedcnt+pavecnt+assumecnt
!
! CONVERT DATE/TIME STAMP TO MINUTES USING FUNCTION
!
       mtime(i)=convert_date2min (yy,m,dd,hr,min)
!
! QUALITY CONTROL FOR CHRONOLOGICAL ORDER
!
       if (mtime(i) .le. savetime) then
          print *, yy,mm,dd,hr,min, '—is out of order'
          ierrcnt=ierrcnt+1
                                    endif
       savetime=mtime(i)
    enddo
      print *, 'maxnum exceeds', maxnum
      stop 16
9 nvalues=i-1
    print *, 'Function date2minute has been completed successfully!'
    if (errorcnt .gt. 0) then
     print *, 'Stopping due to', errorcnt, 'error(s) in the meteorological assumptions'
     stop 17
                        endif
    if (ierrcnt .gt. 0) then
     print *, 'Stopping due to', ierrcnt, 'error(s)'
     stop 18
                      endif
    print *, 'Quality control procedures completed successfully!'
```

```
!
! CALCULATE INTERVAL DIFFERENCES FOR PARAMETERS
!
  do i=1,nvalues-1
     dt=mtime(i+1)-mtime(i)
     ar=air(i+1)-air(i)
     slopeair=ar/dt
     dw=dew(i+1)-dew(i)
     slopedew=dw/dt
     spd=speed(i+1)-speed(i)
     slopespeed=spd/dt
     p=pave(i+1)-pave(i)
     slopepave=p/dt
!
! CREATE ONE MINUTE INTERPOLATION VALUES FOR PARAMETERS
!
     call lin_inter  (dt,mtime(i),air(i),slopeair,dew(i),slopedew,speed(i), slopespeed,pave(i),  &
                      slopepave,newmin,TTA,TTD,WWS,TTP,ict,maxdim)
  enddo
!
! TAKE CARE OF FINAL DATA POINT
!
      ict=ict+1
      m=ict
      TTA(m)=air(nvalues)
      TTD(m)=dew(nvalues)
      WWS(m)=speed(nvalues)
      TTP(m)=pave(nvalues)
      newmin(m)=mtime(nvalues)
   print *, 'Linear interpolation completed successfully!'
!
! ECHO BACK ALL OF MY MINUTE BY MINUTE DATA TO THE SCREEN
!
  write(201,*)   'Date      Time        Depth             TFD'
  TFD=0.d0
  do m=1,ict
     call accumulation (TTA(m),TTD(m),WWS(m),TTP(m),m,smr,R,Rsmr,depth,TFD,  &
                        cela,Ka,celd,Kd,sd,celp,Kp,b,c,D,D1,D2)
     call convert_min2date  (newmin(m),yyy,mmm,ddd,hhh,mmin)
!
! USING LINEAR LOGISTIC REGRESSION TO DETERMINE PROBABILITY (P) OF
! OBSERVING A PREDICTED FROST DEPTH (TFD)
!
      prob=1.d0/((1.d0+exp(-(-3.0575d0+(296.9d0*TFD)))))
!
! PRINT TO OUTPUT FILE (OUTPUT1)
!
      write(201,101) yyy,mmm,ddd,hhh,mmin,depth,TFD,prob
101  format (3i2.2,1x,2i2.2,1x,2f14.8,1x,f6.4)
   enddo
   print *,'Completed frost accumulation process successfully!'
   print *,'You have created one output file.  Check out the following file:'
```

```
  print *,'                                output1'
!
! CLOSING FILES...END OF DRIVER PROGRAM
!
  close (unit=200)
  close (unit=201)
  stop
  end
!
  function convert_date2min (yy,mm,dd,hr,min)
!
! THIS IS A FORTRAN 90 FUNCTION PROGRAM. THE PURPOSE OF THIS
! FUNCTION IS TO TAKE A CALENDAR DATE AND TIME STAMP AND CONVERT
! INTO TOTAL MINUTES. THIS FUNCTION TAKES INTO ACCOUNT THE YEAR
! 2000 CHANGE OVER AND LEAP YEAR ISSUES. A REFERENCE CALENDAR DATE
! (01/01/93) IS USED.  THIS FUNCTION HAS DATA BOUNDS FROM 1993 TO 2020.
! IF YOU NEED TO USE DATA OUTSIDE THESE BOUNDS...THE FUNCTION
! NEEDS TO BE ADJUSTED ACCORDINGLY IN A COUPLE OF LOCATIONS
! WITHIN THIS PROGRAM. THIS FUNCTION QUALITY CONTROLS THE DATA
! INCOMING AND WHEN AN ERROR IS FOUND...THE PROGRAM STOPS AND
! PRINTS LOCATION OF ERROR.  THE CALCULATIONS IN THIS FUNCTION ARE
! ROUTED BACK TO THE DRIVER PROGRAM. THIS PROGRAM WAS CREATED
! BY DAVID KNOLLHOFF (AUGUST 2000).
!
! DEFINITIONS
!
! convert_date2min      = total minutes value for the calendar day and 24 hour time period
! year                  = dummy variable for yy read in
! leapyrs               = to determine if your year falls in a four year period
! totdays               = calculation of number of days since Jan 1 1993
! tdinmo                = variable to account for leap year extra day in February
! lymo                  = leap year month (total of days possible)
! nlymo                 = non leap year month (total of days possible)
! dinmo                 = days in non leap year month
!
! INITIALIZATION
!
  implicit none
  integer convert_date2min
  integer yy,mm,dd,hr,min
  integer year,leapyrs,totdays,tdinmo
  integer lymo(12),nlymo(12),dinmo(12)
  data lymo   /0,31,60,91,121,152,182,213,244,274,305,335/
  data nlymo  /0,31,59,90,120,151,181,212,243,273,304,334/
  data dinmo  /31,28,31,30,31,30,31,31,30,31,30,31/
  year=yy
```

```
!
! QUALITY CONTROL DATA AND CHECK FOR Y2K
!
  if (year .le. 20) year=year+100                    ! fixup for 2000-2020
  if (year .lt. 93 .or. year .gt. 120) then
   print *, yy,mm,dd,hr,min,' -- YEAR is out of range'
  stop 10
                                    endif
  if (mm .le. 0 .or. mm .gt. 12) then
   print *, yy,mm,dd,hr,min,' -- MONTH is out of range'
  stop 11
                                   endif
  if (dd .le. 0 .or. mm .gt. 31) then
   print *, yy,mm,dd,hr,min,' -- DAY is out of range'
  stop 12
                                  endif
  if (hr .lt. 0 .or. hr .gt. 23) then
   print *, yy,mm,dd,hr,min,' -- HOUR is out of range'
  stop 13
                                 endif
  if (min .le. 0 .or. mm .gt. 12) then
   print *, yy,mm,dd,hr,min,' -- MINUTES is out of range'
  stop 14
                                   endif
!
! CHECK FOR LEAP YEARS
!
  leapyrs=(year-93)/4                                ! for 'prior full years'
  totdays=365*(year-93)+leapyrs                      ! with correction for leap years
  if (mod(year-92,4) .eq. 0) then
     tdinmo=dinmo(mm)                                ! we've got leap year
     if (mm .eq. 2) tdinmo=29
     if (dd .le. 0 .or. dd .gt. tdinmo) then
      print *, yy,mm,dd,hr,min,' -- DAY is out of range'
      stop 14
                                     endif
     totdays=totdays+lymo(mm)                        !  months prior to mm – leap year
                                   else              !  not a leap year
  if (dd .le. 0 .or. dd .gt. dinmo(mm)) then
   print *, yy,mm,dd,hr,min,' – DAY is out of range'
   stop 15
                                       endif
  totdays=totdays+nlymo(mm)                          !  month prior to mm -- not a leap year
                                  endif
!
! CALCULATE MINUTES SINCE JANUARY 1, 1993 (01/01/93)
!
  totdays=totdays+dd-1
  convert_date2min=1440*totdays+60*hr+min     !  calculated minutes
  return
  end
!
```

```
      subroutine lin_inter (NN,MT,TA,SA,TD,SD,WS,SS,TP,SP,newmin,TTA,TTD,WWS,TTP, &
                            ict,maxdim)
!
! THIS IS A FORTRAN 90 SUBROUTINE TO CALCULATE THE MINUTE BY
! MINUTE VALUES FOR 2-M AIR TEMPERATURE...2-M DEW POINT
! TEMPERATURE...5-M WIND SPEED AND PAVEMENT TEMPERATURE DATA.
! THIS SUBROUTINE IS CALLED IN THE DRIVER PROGRAM PORTION.  THIS
! PROGRAM WAS CREATED BY DAVID KNOLLHOFF (AUGUST 2000).
!
! DEFINITIONS
!
! newmin      = interpolated values of time stamp
! TTA         = interpolated values of air temperature
! TTD         = interpolated values of dew point temperature
! WWS         = interpolated values of wind speed
! TTP         = interpolated values of pavement temperature
! i           = loop counter
!
! INITIALIZATION
!
! NN=dt
! MT=mtime(i)
! TA=air(i)
! SA=slopeair(i)
! TD=dew(i)
! SD=slopedew
! WS=speed(i)
! SS=slopespeed
! TP=pave(i)
! SP=slopepave
      implicit none
      integer i,m,ict,maxdim
      integer NN,MT,newmin(maxdim)
      real*8 TA,SA,TD,SD,WS,SS,TP,SP
      real*8 TTA(maxdim),TTD(maxdim),WWS(maxdim),TTP(maxdim)
!
! CREATE ONE MINUTE VALUES
!
      do I=1,NN
        ict=ict+1
        if (ict .gt. maxdim) then
          print *, 'maxdim too small – STOP – maxdim=', maxdim
          stop 222
                              endif
        m=ict
        TTA(m)=SA*(i-1)+TA
        TTD(m)=SD*(i-1)+TD
        WWS(m)=SS*(i-1)+WS
        TTP(m)=SP*(i-1)+TP
        newmin(m)=MT+i-1
```

```
  enddo
  return
  end
!
  subroutine accumulation (IA,ID,IS,IP,ii,smr,R,Rsmr,depth,TFD,cela,Ka,celd,Kd,sped, &
                           celp,Kd,sped,celp,Kp,b,c,D,D1,D2)
!
! THIS IS A FORTRAN 90 SUBROUTINE THAT WILL CALCULATE (PREDICT) THE
! TOTAL DEPTH OF FROST WITH TIME.  THE ONE MINUTE LINEARLY
! INTERPOLATED VALUES ARE USED IN THE ACCUMULATION PROCESS.  THE
! RATE OF SNOW MELT IS TAKEN INTO ACCOUNT WHEN PAVEMENT
! TEMPERATURES RISE OR REMAIN ABOVE 32 F. MODEL INPUT NEEDS TO BE
! IN INCREMENTS OF 1 MINUTE INTERPOLATED VALUES TO RUN MODEL
! CALCULATIONS PROPERLY.  PRECITATION IS NOT TAKEN INTO ACCOUNT.
! EVAPORATION OF FROST IS ALLOWED WITH MELTING...BUT DEPOSITION
! OF MOISTURE IS NOT ALLOWED DURING MELTING PERIODS.
!
! DEFINTIONS                                                          UNITS
!
! roui      = density of ice @ 32 F                                   kgm^-3
! eps       = epsilon-ration of molecular weights of H2O/dry air      no units
! ce        = transfer coefficient                                    no units
! Rd        = gas constant for dry air                                Jkg^-1K^-1
! esTo      = saturation vapor pressure at the freezing point         Pa
! Ld        = latent heat of deposition at the freezing point         Jkg^-1
! Rv        = gas constant for water vapor                            Jkg^-1K^-1
! To        = freezing point temperature                              K
! IA        = interpolated air temperatures                           F
! ID        = interpolated dew point temperatures                     F
! IS        = interpolated wind speed values                          Mph
! IP        = interpolated pavement temperatures                      F
! const     = constant given the stability of the air is fixed        K
! const1    = ratio of latent heat of deposition at the freezing point over the   K
!             specific gas constant for dry air
! D1        = exponential function of the saturation vapor pressures for the 2-m  no units
!             dew point temperatures
! D2        = exponential function of the saturation vapor pressures for 2-m      no units
!             pavement temperatures
! D         = the difference of the two exponential functions         no units
! R         = frost deposition/evaporation/sublimation rate           mmmin^-1
! a         = inverse ratio of freezing point temperature             K^-1
! celp      = pavement temperature converted from °F into °C          C
! Kp        = pavement temperature converted from °C into kelvin      K
! cela      = 2-m air temperature converted from °F into °C           C
! Ka        = 2-m air temperature converted from °C into kelvin       K
! celd      = 2-m dew point temperature converted from °F into °C     C
! Kd        = 2-m dew point temperature converted from °C into kelvin K
! sped      = 5-m wind speed values converted from mph in ms^-1       ms^-1
! b         = calculation of inverse ratio of dew point temperatures  K^-1
! c         = calculation of inverse ratio of pavement temperatures   K^-1
! depth     = frost accumulation depth                                mm
! TFD       = total frost accumulation                                mm
```

```
! e          = constant for snow melt equation                          no units
! f          = constant for snow melt equation                          no units
! smr        = snow melt rate (taken from ETA model)                    ms-1
! Rsmr       = calculation of deposition or sublimation                 mmmin-1
!
! INTIALIZATION
!
! IA=TTA(m)
! ID=TTD(m)
! IS=WWS(m)
! IP=TTP(m)
! ii=m
  implicit none
  real*8 roui,eps,ce,Rd,esTo,Ld,Rv,To,e,f,a,const,const1,D1,D2,D,b,c
  real*8 celp,Kp,cela,Ka,celd,Kd,sped
  real*8 smr,R,Rsmr,depth,TFD,tdepth
  real*8 IA,ID,IS,IP
  integer ii
!
! CHECK WIND SPEED
!
          if (IS .eq. 0.d0) then
             IS=1.d0
                          endif
!
! CONSTANTS
!
  roui  = 917
  eps   = 0.622d0
  ce    = 0.001d0
  Rd    = 287.0d0
  EsTo  = 610.8d0
  Ld    = 2834000.0d0
  Rv    = 461.0d0
  To    = 273.16d0
! e is multiplied by 1000 mm for unit conversions for smr which is originally in units of ms-1.
! This is a more convenient location to do the conversion than down below.
! e = 1.0513*0.00000001*1000.
  e = 1.0513d-5
  f = 0.0000000648d0
!
! CONVERSION OF TEMPERATURES (from °F to °C to kelvin)
!
   cela = (IA-32.d0)/1.8d0
   Ka = cela+273.16d0
!
   celd = (ID –32.d0)/1.8d0
   Kd = celd+273.16d0
!
   celp = (IP-32.d0)/1.8d0
   Kp = celp+273.16d0
!
```

```
! CONVERSION OF WIND SPEEDS (from mph to ms-1)
!
  sped = IS*0.44704d0
!
! MODEL:  VAPOR PRESSURES, FROST RATES, DEPTH, AND TOTAL DEPTH
!
        if (Kp .eq. Kd) then
           Kd=Kp+0.10d0
                        endif
! const=(eps/roui)*ce*(esTo/Rd)
         const=0.000001443d0
! const1=Ld/Rv
         const1=6147.505423d0
  a=1./To
     a=0.003660858d0
     b=1.d0/Kd
     c=1.d0/Kp
     D1=exp(const1*(a-b))
     D2=exp(const1*(a-c))
     D=D1-D2
!
! When multiplied by 60. seconds = 1 minute
! When multiplied by 1000. Mm = 1 meter
!
! Snow melt rate (smr) is assumed to be in units of (ms-1) then multiplied by 60s/min and by
! 1000 mm to get final units of mmmin-1 for smr and Rsmr
!
! Rate of deposition (sublimation) or evaporation of moisture (R) has units of (mmmin-1) for
! each interpolated value.
!
   if (Kp .gt. 273.16d0 .and. D .lt. 0.d0) then
! Scenario #1 melting and evaporation
    smr=-(10.d0*e*((Kp-273.16d0)*(((Kp**4)*f)+1.d0))/Kp))*60.d0
    R=1000.d0*(const*(sped/Ka)*D*60.d0)
    Rsmr=(R+(smr))
   elseif (Kp .gt. 273.16d0 .and. D .gt. 0.d0) then
! Scenario #2 melting only allowed, Not deposition
    smr=-(10.d0*e*((Kp-273.16d0)*(((Kp**4)*f)+1.d0))/Kp))*60.d0
    R=1000.d0*(const*(sped/Ka)*D*60.d0)
   Rsmr=smr
   elseif (Kp .le. 273.16d0 .and. D .lt. 0.d0) then
! Scenario #3 Evaporation/sublimation , no melting allowed
   smr=0.d0
    R=1000.d0*(const*(sped/Ka)*D*60.d0)
   Rsmr=R
   elseif (Kp .le. 273.16d0 .and. D .gt. 0.d0) then
! Scenario #4 Deposition, no melting allowed
   smr=0.d0
    R=1000.d0*(const*(sped/Ka)*D*60.d0)
   Rsmr=R
                                        endif
!
```

```
! CALCULATION OF FROST ACCUMULATION DEPTHS (depth)
!
! Because 1 minute interpolated values are used, Rsmr is multiplied by a delta time of 1
! minute to satisfy unit cohesiveness for depth (mm)
!
      if (ii .eq. 1) then
         depth=0.d0
                  else
         depth=(Rsmr*1.d0)
                  endif
!
! CALCULATION OF TOTAL FROST DEPTHS (TFD)
!
       TFD=TFD+depth
       if (TFD .lt. 0.d0) then
          TFD=0.d0
                        endif
       return
       end
!
  subroutine convert_min2date (minutes_in,year,month,day,hour,min)
!
! THIS IS A SUBROUTINE PROGRAM TO TAKE THE NUMBER OF MINUTES AND
! CONVERT BACK TO CALENDAR DATE AND TIME STAMP IN HOURS AND
! MINUTES.  THE PROGRAM TAKES INTO ACCOUNT LEAP YEARS AND
! TRANSITION AROUND Y2K.  ONCE THE CORRECT YEAR HAS BEEN
! DETERMINED...THE PROGRAM WORKS DOWN BY A PROCESS OF
! ELIMINATION TO GET MONTH...DAY...HOUR...AND MINUTE.  NO QUALITY
! CONTROL IS NEEDED IN THIS SECTION.  THE PROGRAM WAS CREATED BY
! DAVID KNOLLHOFF (AUGUST 2000).
!
! DEFINITIONS
!
! minutes_in   = dummy variable for total minutes since 1/1/93
! minutes      = variable for total minutes since 1/1/93
! min          = final number minutes left for time stamp
! mn1          = calculation of final minutes
! month        = final number for month left in date stamp
! m4yr         = calculation to determine what four year period
! m1yr         = number of minutes in four year period
! m4           = ratio of number of minutes in four year period
! m1           = ratio of number of minutes in one year
! mm1          = month of interest
! lymo         = number of days in leap year month
! nlymo        = number of days in non leap year month
! year         = year of interest
! yy1          = calculation of year of interest
! numday       = ratio of number of days
! dd1          = calculation of day of interest
! day          = day of interest
! hh1          = calculation of hours of interest
! hour         = hour of interest
```

```
!
! INITIALIZATION
!
  implicit none
  integer minutes,min,mn1,month,dd1,day,hh1,hour,minutes_in
  integer year, yy1,m4yr,m1yr,m4,m1,numday,mm1
  integer lymo(12),nlymo(12)
  data lymo  /0,31,60,91,121,152,182,213,244,274,305,335/
  data nlymo /0,31,59,90,120,151,181,212,243,273,304,334/
  minutes=minutes_in
!
! CONVERT MINUTES TO CALENDAR DATES SINCE JAN 1, 1993 (1/1/93)
!
! What year are we in?
   m4yr=((4*365)+1)+1440
   m1yr=365*1440
   m4=minutes/m4yr
   minutes=minutes-(m4*m4yr)
   m1=minutes/m1yr
   if (m1 .eq. 4) then                ! correct for last day of leap year
       m1 = 3
                  endif
  minutes=minutes-(m1*m1yr)
   yy1=93+(m4*4)+m1
  if (yy1 .ge. 100) then              ! adjust for the transition to 2000+
      yy1=yy1-100
                    endif
  year=yy1                            ! Our answer has been found for year
!
! What month are we in?
!
   numday=minutes/1440                ! number of full days
   if (m1 .eq. 3) then                ! leap year
      do mm1= 12,1,-1
       if (lymo(mm1) .le. numday) exit
      enddo
      minutes=minutes-(lymo(mm1)*1440
                  else                ! not a leap year
      do mm1 = 12,1,-1
       if (nlymo(mm1) .le. numday) exit
      enddo
      minutes=minutes-(nlymo(mm1)*1440)
                  endif
   month=mm1                          ! Our answer has been found for month
!
! What day are we in?
!
   numday=minutes/1440                ! number of full days
   dd1=numday+1
   day=dd1                            ! Our answer has been found for day
  minutes=minutes-(numday*1440)
!
```

```
! What hour are we in?
!
   hh1=minutes/60
   hour=hh1                    ! Our answer has been found for hour
!
! What minutes are we in?
!
   mn1=minutes-(hh1*60)
   min=mn1                     ! Our answer has been found for minutes
   return
   end
```

APPENDIX C. POSITIVE MODEL FROST ACCUMULATION CASES

Case Study	Frost Depth (mm)	(-) Natural Log	Observation
Mason City			
1	0.00726	4.93	Y
2	0.01586	4.14	Y
3	0.07045	2.65	Y
4	0.03371	3.39	Y
5	0.00605	5.11	Y
6	0.05974	2.82	Y
7	0.00462	5.38	Y
8	0.03874	3.25	Y
9	0.0001	9.21	N
10	0.00068	7.29	N
11	0.00677	5.00	N
12	0.002	6.21	N
13	0.00071	7.25	N
14	0.0001	9.21	N
Spencer			
15	0.01431	4.25	Y
16	0.01116	4.50	Y
17	0.01033	4.57	Y
Waterloo			
18	0.0032	5.74	Y
19	0.0029	5.84	Y

20	0.0415	3.18	Y
21	0.01772	4.03	Y
22	0.0557	2.89	Y
23	0.00748	4.90	Y
24	0.0003	8.11	Y
25	0.00578	5.15	Y
26	0.03375	3.39	Y
27	0.02264	3.79	Y
28	0.01179	4.44	Y
29	0.0001	9.21	Y
30	0.02926	3.53	Y
31	0.0001	9.21	Y
32	0.00858	4.76	N
33	0.00641	5.05	N
34	0.0003	8.11	N
35	0.0001	9.21	N
36	0.00011	9.12	N
37	0.01635	4.11	N
38	0.02022	3.90	N
Ames			
39	0.02058	3.88	Y
40	0.01838	4.00	Y
41	0.00375	5.59	Y
42	0.00289	5.85	Y
43	0.00067	7.31	Y

44	0.01099	4.51	Y
45	0.0001	9.21	Y
46	0.01214	4.41	Y
47	0.05368	2.92	Y
48	0.05371	2.92	Y
49	0.0003	8.11	Y
50	0.00569	5.17	Y
51	0.00167	6.39	N
52	0.002	6.21	N
53	0.00172	6.37	N
54	0.00072	7.24	N
55	0.00306	5.79	N
56	0.00063	7.37	N
57	0.00004	7.82	N
58	0.002	6.21	N
59	0.00108	6.83	N
60	0.009	4.71	N
61	0.00994	4.61	N
62	0.00468	5.36	N
63	0.0002	8.52	N
64	0.00505	5.29	N
65	0.0061	5.10	N
66	0.00074	7.21	N
67	0.002	6.21	N
68	0.00385	5.56	N

Des Moines			
69	0.0115	4.47	Y
70	0.001	6.91	Y
71	0.0049	5.32	Y
72	0.067	2.70	Y
73	0.0094	4.67	Y
74	0.00084	7.08	N
75	0.00058	7.45	N
76	0.00146	6.53	N
77	0.007	4.96	N
78	0.01951	3.94	N
79	0.00094	6.97	N
80	0.0002	8.52	N
81	0.01393	4.27	N
82	0.00064	7.35	N
83	0.00001	11.51	N
84	0.00943	4.66	N
85	0.0001	9.21	N
86	0.0044	5.43	N
87	0.00001	11.51	N
88	0.00026	8.25	N

APPENDIX D. CONTINGENCY TABLES FOR THE VARIOUS FROST DEPTHS

Threshold frost depth = 0.00 mm		Iowa DOT frost observations	
		Yes	No
Frost model forecast	Yes	A = 42	B = 46
	No	C = 6	D = 368

H = A/(A+C) = 0.875
FAR1 = B/(A+B) = 0.523
FAR2 = B/(B+D) = 0.111

Threshold frost depth = 0.00001 mm		Iowa DOT frost observations	
		Yes	No
Frost model forecast	Yes	A = 42	B = 44
	No	C = 6	D = 370

H = A/(A+C) = 0.875
FAR1 = B/(A+B) = 0.512
FAR2 = B/(B+D) = 0.106

Threshold frost depth = 0.0001 mm		Iowa DOT frost observations	
		Yes	No
Frost model forecast	Yes	A = 39	B = 39
	No	C = 9	D = 375

H = A/(A+C) = 0.813
FAR1 = B/(A+B) = 0.500
FAR2 = B/(B+D) = 0.094

Threshold frost depth = 0.000335 mm		Iowa DOT frost observations	
		Yes	No
Frost model forecast	Yes	A = 37	B = 35
	No	C = 11	D = 379

H = A/(A+C) = 0.771
FAR1 = B/(A+B) = 0.486
FAR2 = B/(B+D) = 0.085

Threshold frost depth = 0.001 mm		Iowa DOT frost observations	
		Yes	No
Frost model forecast	Yes	A = 35	B = 26
	No	C = 13	D = 388

H = A/(A+C) = 0.729
FAR1 = B/(A+B) = 0.426
FAR2 = B/(B+D) = 0.063

Threshold frost depth = 0.002 mm		Iowa DOT frost observations	
		Yes	No
Frost model forecast	Yes	A = 35	B = 18
	No	C = 13	D = 396

H = A/(A+C) = 0.729
FAR1 = B/(A+B) = 0.340
FAR2 = B/(B+D) = 0.043

Threshold frost depth = 0.007 mm		Iowa DOT frost observations	
		Yes	No
Frost model forecast	Yes	A = 26	B = 9
	No	C = 22	D = 405

H = A/(A+C) = 0.542
FAR1 = B/(A+B) = 0.257
FAR2 = B/(B+D) = 0.022

Threshold frost depth = 0.018 mm		Iowa DOT frost observations	
		Yes	No
Frost model forecast	Yes	A = 13	B = 2
	No	C = 35	D = 412

H = A/(A+C) = 0.271
FAR1 = B/(A+B) = 0.133
FAR2 = B/(B+D) = 0.005

REFERENCES

Agresti, A., 1984: *Analysis of Ordinal Categorical Data.* Wiley & Sons, Inc., 287 pp.

Aitchison, J., and S. D. Silvey, 1957: The generalization of probit analysis to the case of multiple responses. *Biometrika*, **44**, 131-140.

Ashford, J. R., 1959: An approach to the analysis of data for semi-quantal responses in biological assay. *Biometrics*, **15**, 573-581.

Barker, H. W., and J. A. Davies, 1990: Formation of ice on roads beneath bridges. *J. Appl. Meteor.*, **29**, 1180-1184.

Bogren, J., 1991: Screening effects on road surface temperature and road slipperiness. *Theor. Appl. Climatol.*, **43**, 91-99.

Bogren, J., and T. Gustavsson, 1989: Modeling of local climate for prediction of road slipperiness. *Phys. Geogr.*, **10**, 147-164.

Bogren, J., and T. Gustavsson, 1991: Nocturnal air and road surface temperature variations in complex terrain. *Int. J. Climatol.*, **11**, 443-455.

Bogren, J., T. Gustavsson, and S. Lindqvist, 1992: A description of a local climatological model used to predict temperature variations along stretches of road. *Meteor. Mag.*, **121**, 157-164.

Buizza, R., A. Hollingsworth, F. Lalaurette, and A. Ghelli, 1999: Probabilistic predictions of precipitation using the ECMWF Ensemble Prediction System. *Wea. Forecasting,* **14**, 168-189.

Buizza, R., A. Hollingsworth, F. Lalaurette, and A. Ghelli, 2000: Reply to comments by Wilson and by Juras. *Wea. Forecasting,* **15**, 367-369.

Cox, D. R., and E. J. Snell, 1989: *The Analysis of Binary Data, 2nd Edition.* Chapman and Hall, 236 pp.

Freeman, D.H., Jr., 1987: *Applied Categorical Data Analysis.* Marcel Dekker, Inc.

Green, D. M., and J. A. Swets, 1974: *Signal Detection Theory and Psychophics.* Wiley and Sons, Inc., 455 pp.

Gustavsson, T., 1990: Variation in road surface temperature due to topography and wind. *Theor. Appl. Climatol.*, **41**, 227-236.

Gustavsson, T., 1991: Analyses of local climatological factors controlling risk of road slipperiness during warm-air advections. *Int. J. Climatol.*, **11**, 315-330.

Gustavsson, T., and J. Bogren, 1990: Road slipperiness during warm-air advections. *Meteor. Mag.,* **119**, 267-270.

Gustavsson, T. and J. Bogren, 1993: Evaluation of a local climatological model test carried out in the county of Halland, Sweden. *Meteor. Mag.*, **122**, 257-267.

Hewson, T. D., and N.J. Gait, 1992: Hoar-frost deposition on roads. *Meteor. Mag.*, **121**, 1-21.

Hosmer, D.W., Jr., and Lemeshow, S., 1989: *Applied Logistic Regression*. Wiley & Sons, Inc.

Juras, J., 2000: Comments on "Probabilistic predictions of precipitation using the ECMWF Ensemble Prediction System." *Wea. Forecasting*, **15**, 365-366.

Katsoulis, B., and G. Theoharatos, 1985: Indications of the urban heat island in Athens, Greece. *J. Clim. Appl. Meteor.*, **24**, 1296-1302.

Marzban, C., 1998: Scalar measures of performance in rare-event situations. *Wea. Forecasting*, **13**, 753-763.

Mason, I., 1982a: On scores for yes/no forecasts. *Proceedings of Ninth Conference Weather Forecasting and Analysis*, Amer. Meteor. Soc., 169-174.

Mason, I., 1982b: A model for assessment of weather forecasts. *Aust. Meteor. Mag.*, **30**, 291-303.

McCoy, M. C., 1986: Severe-storm-forecast results from PROFS 1983 forecast experiment. *Bull. Amer. Meteor. Soc.*, **67**, 155-164.

Nichols, C., 1999: Frost deposition on roadways: refinement of a simple model. Undergraduate Senior Thesis, Iowa State University, Dept. of Geol. and Atmos. Sci., 1-6.

Oke, T., 1978: *Boundary Layer Climates*. Halsted Press, 435 pp.

Oke, T., 1982: The energetic basis of the urban heat island. *Quart. J. Roy. Meteor. Soc.*, **108**, 1-24.

Rayer, P. J., 1987: The Meteorological Office forecast road surface temperature model. *Meteor. Mag.*, **116**, 180-191.

Sass, B. H., 1992: A numerical model for prediction of road temperature and ice. *J. Appl. Meteor.*, **31**, 1499-1506.

Sass, B. H., 1997: A numerical forecasting system for the prediction of slippery roads. *J. Appl. Meteor.*, **36**, 801-817.

Shao, B., 1990: A winter road surface temperature prediction model with comparison to others. Ph.D. thesis, The University of Birmingham, 245 pp.

Shao, J., and P. J. Lister, 1996: An automated nowcasting model of road surface temperature and state for winter road maintenance. *J. Appl. Meteor.*, **35**, 1352-1361.

Shao, J., and P. J. Lister, 1998: Short and medium term road ice predictions for winter road maintenance. *Appl. Tech. II*, **10**, 1-14.

Shao, J., P. J. Lister, G. D. Hart, and H. B. Pearson, 1997: Thermal mapping: reliability and repeatability. *Meteor. Appl.*, **4**, 325-330.

Shao, J., J. C. Swanson, R. Patterson, P. J. Lister, and A. N. McDonald, 1998: Variation of winter road surface temperature due to topography and application of thermal mapping. *Meteor. Appl.*, **5**, 131-137.

Stull, R. B., 1988: *An Introduction to Boundary Layer Meteorology*. Kluwer Academic Publishers, 670 pp.

Swets, J. A., 1973: The relative operating characteristic in psychology. *Science*, **182**, 990-999.

Swets, J.A., 1986: Indices of discrimination or diagnostic accuracy: Their ROCS and implied models. *Psychol. Bull.*, **99**, 100-117.

Swets, J.A., 1988: Measuring the accuracy of diagnostic systems. *Science*, **240**, 1285-1293.

Takle, E. S., 1990: Bridge and roadway frost: occurrence and prediction by use of an expert system. *J. Appl. Meteor.*, **29**, 727-734.

Thornes, J. E., 1989: A preliminary performance and benefit analysis of the UK national road ice prediction system. *Meteor. Mag.*, **118**, 93-99.

Thornes, J. E., and J. Shao, 1991: Spectral analysis and sensitivity tests for a numerical road surface temperature prediction model. *Meteor. Mag.*, **120**, 117-120.

Thornes, J. E., 1996: The quality and accuracy of a sample of public and commercial weather forecasts in the UK. *Meteor. Appl.*, **3**, 63-74.

Wilks, D. S., 1995: *Statistical Methods in the Atmospheric Sciences*. Academic Press, 467 pp.

Wilson, L. J., 2000: Comments on "Probabilistic predictions of precipitation using the ECMWF Ensemble Prediction System." *Wea. Forecasting*, **15**, 361-364.

ACKNOWLEGDEMENTS

I would like to take this opportunity to express my many thanks and gratitude to those individuals and agencies who have assisted me toward the completion of my graduate program at Iowa State University.

First, I would like to thank my advisors Dr. E. Takle and Dr. W. Gallus for their support and patience. I would also like to extend my thanks to my committee member Dr. R. Arritt for his encouragement and challenges throughout the graduate process.

My thanks also go to Iowa State University employees Mr. C. Anderson for having provided computer programming and statistical assistance whenever problems arose, and Dr. D. Todey for his helpful advice with technical issues.

I can not forget to thank my fellow National Weather Service Des Moines office co-workers. You all are great. Thanks for the late-night pep talks and the many laughs.

My thanks also go to my fellow graduate and undergraduate students in meteorology, Seth Loyd, Jinho Yoon, Kathryn St. Croix, Jerimiah Birdsall, Jared Anderson, Brad Temeyer, who have shared their joys and tears with me and have made the third floor of Agronomy Hall feel more like home.

I extend my many thanks and hugs to my family for their consistent involvement and encouragement through the good times and the difficult times.

Finally I would like to thank the auspices of the Iowa Department of Transportation for funding my salary as a graduate research assistant. More specifically, Mr. D. Burkheimer and Ms. D. McCauley from the Winter Maintenance Division at the Iowa DOT deserve many thanks for their direct involvement in data gathering processes. Their time and efforts are much appreciated. Without the financial and technical support from the Iowa DOT, the completion of my graduate program would not have been possible. I would like to say thanks.

BIOGRAPHICAL SKETCH

David Scott Knollhoff was born January 15, 1972 in Peoria, Illinois. He received the Bachelor of Science degree in Meteorology from Florida State University in 1996. He served as a research assistant in the Department of Meteorology. His job was to maintain a database for local seabreeze experimental data while attending Florida State University. After graduation, he served as an on-site weather forecaster for the PGA Tour before attending graduate school at Iowa State University. He served as a research assistant in the Department of Geological and Atmospheric Sciences at Iowa State University from February,1997 through April, 1999 studying pavement temperatures and frost formation on roadways and bridges. Prior to graduation he was hired as a meteorological intern at the Des Moines National Weather Service Forecast Office in April, 1999.